4-2012

An Analysis of Multiple Predecessor Rain Events ahead of Tropical Cyclones Ike and Lowell: 10–15 September 2008

Lance F. Bosart
University at Albany, State University of New York, bosart@atmos.albany.edu

Jason M. Cordeira
University at Albany, State University of New York

Thomas J. Galarneau Jr.
National Center for Atmospheric Research

Benjamin J. Moore
University of Colorado

Heather M. Archambault
Naval Postgraduate School

An Analysis of Multiple Predecessor Rain Events ahead of Tropical Cyclones Ike and Lowell: 10–15 September 2008

LANCE F. BOSART AND JASON M. CORDEIRA

Department of Atmospheric and Environmental Sciences, University at Albany, State University of New York, Albany, New York

THOMAS J. GALARNEAU JR.

National Center for Atmospheric Research, Boulder, Colorado*

BENJAMIN J. MOORE

Cooperative Institute for Research in Environmental Sciences, University of Colorado, and NOAA/Earth Systems Research Laboratory, Physical Sciences Division, Boulder, Colorado

HEATHER M. ARCHAMBAULT

Naval Postgraduate School, Monterey, California

(Manuscript received 30 June 2011, in final form 16 October 2011)

ABSTRACT

An analysis of three predecessor rain events (PREs) that occurred ahead of North Atlantic tropical cyclone (TC) Ike and east Pacific TC Lowell during 10–15 September 2008 is presented. The three PREs produced all-time daily record rainfall at many locations, including Lubbock, Texas (189.5 mm); Wichita, Kansas (262 mm); and Chicago–O'Hare, Illinois (169 mm), on 11–13 September, respectively.

PRE 1 organized over Texas on 10 September with moisture from a stalled frontal boundary and the Bay of Campeche, and matured with moisture from TC Lowell. PRE 2 organized over the Texas Panhandle on 11 September with moisture from the Bay of Campeche, and developed and matured over Kansas and Missouri with moisture from TC Lowell. PRE 3 developed over Texas on 11 September, merged with and absorbed PRE 2 over Kansas and Missouri, and matured as it ingested moisture from TC Ike. All three PREs matured in the equatorward entrance region of an intensifying subtropical jet stream (STJ).

Heavy rainfall with the three PREs occurred along a plume of moist air characterized by high precipitable water values that extended poleward over the central United States near the juxtaposition of the nose of a low-level jet, a region of lower-tropospheric forcing for ascent along a surface baroclinic zone, and the STJ equatorward entrance region. The cumulative upscale effect of persistent deep convection from the three PREs enhanced and ''locked in'' a favorable upper-tropospheric flow pattern conducive to ridge development over the Ohio Valley and STJ intensification over the central U.S. and Great Lakes region.

1. Introduction

The term predecessor rain event (PRE) was coined by Cote (2007) to describe coherent high-impact flood-producing mesoscale rainstorms that are associated with rainfall rates exceeding 100 mm in 24 h ahead of tropical cyclones (TCs). Composite analyses of PREs by Cote (2007), Galarneau et al. (2010), and Moore (2010) show that PREs typically occur ~1000 km poleward of landfalling

* The National Center for Atmospheric Research is sponsored by the National Science Foundation.

Corresponding author address: Lance F. Bosart, Department of Atmospheric and Environmental Sciences, University at Albany, State University of New York, ES351, 1400 Washington Ave., Albany, NY 12222.
E-mail: bosart@atmos.albany.edu

DOI: 10.1175/MWR-D-11-00163.1

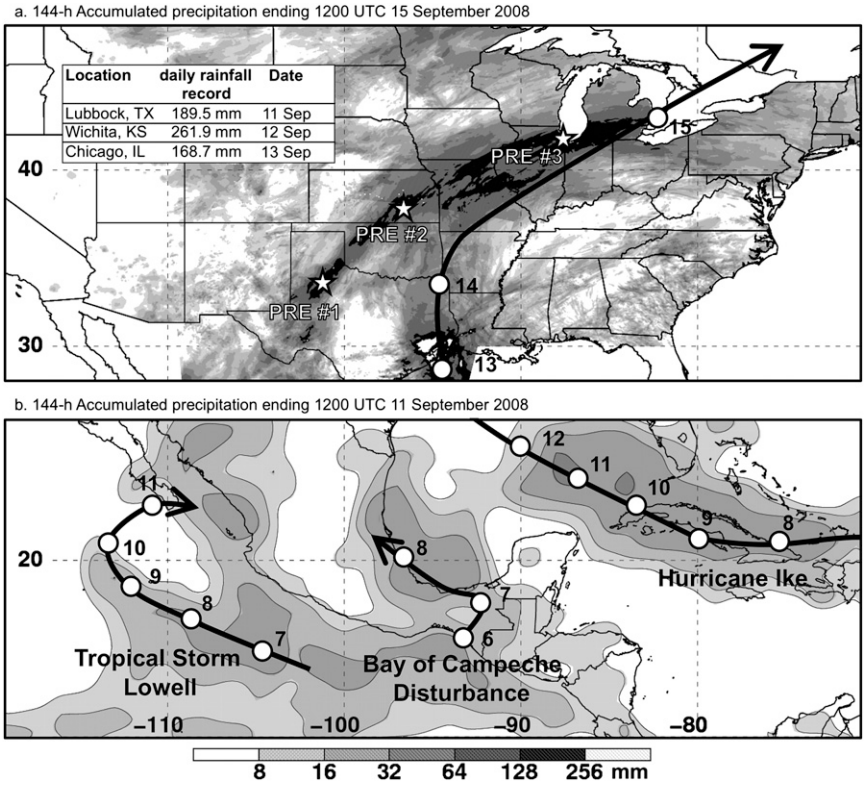

FIG. 1. The 144-h accumulated precipitation ending (a) 1200 UTC 15 Sep 2008 and (b) 1200 UTC 11 Sep 2008. Accumulated precipitation totals are determined from the NPVU QPE analyses in (a) and from the TRMM analyses (degraded to 1.0° × 1.0° horizontal resolution) in (b). Tracks of three systems are shown with 0000 UTC location given by the white filled circles. The approximate locations of precipitation associated with the three PREs are labeled. Daily rainfall records at LBB, ICT, and ORD (locations given by stars) are shown.

TCs. These composite analyses and additional case studies indicate that PREs develop when a plume of tropical moisture emanating from the TC along a low-level jet (LLJ) intersects a quasi-stationary baroclinic zone and is forced to ascend in conjunction with a thermally direct lower-tropospheric frontogenetical circulation in the equatorward entrance region of an upper-tropospheric jet streak (Bosart and Carr 1978; Bosart and Dean 1991; Cote 2007; Galarneau et al. 2010). Under these conditions PREs represent a category of extreme rain-producing mesoscale convective systems (MCSs; e.g., Maddox et al. 1979). A high-impact PRE that involved these processes occurred ahead of TC Erin in August 2007 and produced more than 300 mm of rainfall over southern Minnesota (Galarneau et al. 2010). A numerical modeling analysis of the Erin PRE demonstrated that in the absence of Erin's moisture, the accumulated PRE precipitation over southern Minnesota would be reduced by ~25% (Schumacher et al. 2011).

The twin goals of this study are to investigate the following: 1) multiple moisture source regions that contributed to the development and maturation of three PREs over the central United States ahead of east Pacific TC Lowell and North Atlantic TC Ike during 10–15 September 2008, and 2) the cumulative upscale effect of initial PRE development and associated persistent deep convection on the evolution of the subtropical jet stream (STJ) and subsequent PRE development. The ensuing investigation is motivated by the high-impact nature of three PREs as they contributed to all-time daily record rainfall at Lubbock (LBB), Texas (189.5 mm); Wichita (ICT), Kansas (261.9 mm); and Chicago–O'Hare (ORD), Illinois (168.7 mm)[1], between 10 and 15 September (Fig. 1a). As a point of reference, PRE 1 organized over Texas on 10–11 September, whereas PRE 2 organized over the Texas Panhandle on 11 September and matured over Kansas on 12 September. PRE 3 organized over western Texas on 11 September and extended from the Texas Panhandle northeastward to Missouri on 12 September. The maturation of PRE 3 involved the

[1] A new all-time daily record rainfall of 174.2 mm was set on 23 July 2011 at ORD.

absorption of PRE 2 over Iowa as the rain event progressed over Wisconsin, Illinois, and Indiana on 13 September.

A rainfall estimate constructed from 3-h Tropical Rainfall Measuring Mission (TRMM) analyses for 5–11 September suggests multiple moisture source regions over coastal western Mexico, the Caribbean, and the Gulf of Mexico prior to PRE development (Fig. 1b). These moisture source regions are identified by areas of precipitation associated with a borderline tropical disturbance (hereafter disturbance) over the Bay of Campeche, over eastern Mexico, and southern Texas; TC Lowell over Mexico and western Texas; and TC Ike over the eastern Gulf of Mexico and Cuba. Herein we will show that PRE organization and development occurred in association with *four* key moisture sources, which included high precipitable water (PW) air masses associated with the three previously identified tropical features and an additional high PW air mass aligned along a stalled frontal boundary over the northwestern Gulf of Mexico. Because the disturbance over the Bay of Campeche and the stalled frontal boundary are not TCs, initial PRE development is not consistent with the definition of a PRE as defined by Cote (2007) and Galarneau et al. (2010). However, we will show that the mechanisms responsible for the transport of tropical moisture from these source regions to the central United States and subsequent convective development are consistent with PRE development, and that the maturation of all three PREs involved a TC moisture source.

This paper is organized as follows. Section 2 contains a brief discussion of the data sources. Section 3 presents a large-scale overview and an investigation of the moisture source regions critical to PRE development, whereas section 4 offers a detailed analysis of the mechanisms responsible for PRE organization. Section 5 describes the evolution and maturation of the three PREs and offers preliminary summaries of their life cycles. The interaction of the three PREs with the large-scale environment is documented via cross sections and from a potential vorticity (PV) perspective in section 6. The conclusions follows in section 7.

2. Data sources

Gridded datasets of the National Centers for Environmental Prediction (NCEP) Global Forecast System (GFS) with ~0.5° horizontal grid spacing and 6-h temporal resolution constitute the primary data source for analysis. The NCEP GFS analyses are complemented by Level-II Weather Surveillance Radar-1988 Doppler (WSR-88D) radar reflectivity data collected from the National Climatic Data Center (NCDC), archived upper-level and surface data from the University at Albany, and archived satellite imagery from the Aviation Weather Center–Aviation Digital Data Server (http://aviationweather.gov/adds/). Accumulated precipitation totals are determined from the TRMM 3B42 product (Huffman et al. 2007), National Precipitation Verification Unit (NPVU) quantitative precipitation estimate (QPE) analyses, archived automated surface observation station (ASOS) data at NCDC, and the National Oceanic and Atmospheric Administration (NOAA) Weekly Weather and Crop Bulletin. Air parcel trajectory analyses are computed using the NCEP GFS at 6-h intervals, with linear temporal interpolation used at 2-h intervals between analysis times. Standardized anomalies, used to assess the characteristics of the time-mean circulation, are computed from the long-term (1979–2008) climatology derived from the NCEP–National Center for Atmospheric Research (NCAR) reanalysis (Kalnay et al. 1996) following the methodology of Hart and Grumm (2001).

3. Results: Large-scale overview

a. Time-mean circulation

The large-scale flow regime for 8–14 September 2008 over the continental United States (CONUS) and Central America is characterized by a positively tilted 250-hPa trough over the western CONUS and a downstream 250-hPa ridge that extends from Mexico to the Southeast (Fig. 2a). The 250-hPa temperatures collocated with the 250-hPa ridge exceeded 234 K, representing a standardized departure from climatology >1.5 standard deviations (Fig. 2b). A strong Bermuda anticyclone is centered off the southeast coast at 850 hPa with a relative geopotential height minimum present over the central United States and western Gulf of Mexico and a broad second trough over the Southwest, northwest Mexico, and the adjacent eastern North Pacific (Fig. 2c). The 850-hPa geopotential height minima are likely influenced by the locations of TCs Ike and Lowell during 8–14 September 2008 over the aforementioned respective regions. The observed 850-hPa geopotential height anomalies over the Gulf of Mexico and Caribbean suggest that anomalous lower-tropospheric geostrophic southeasterly flow likely favored the transport of tropical moisture to the central plains and Midwest (Fig. 2c). Likewise, the observed 850-hPa temperature anomalies over the Gulf of Mexico suggest the presence of lower-tropospheric warm-air advection ahead of the central U.S. trough (Fig. 2d).

b. Observed rainfall distribution

The total NPVU-derived accumulated precipitation for the 5-day period ending at 1200 UTC on 15 September shows an anticyclonically curved swath of heavy rainfall over the central and northern CONUS consisting of two

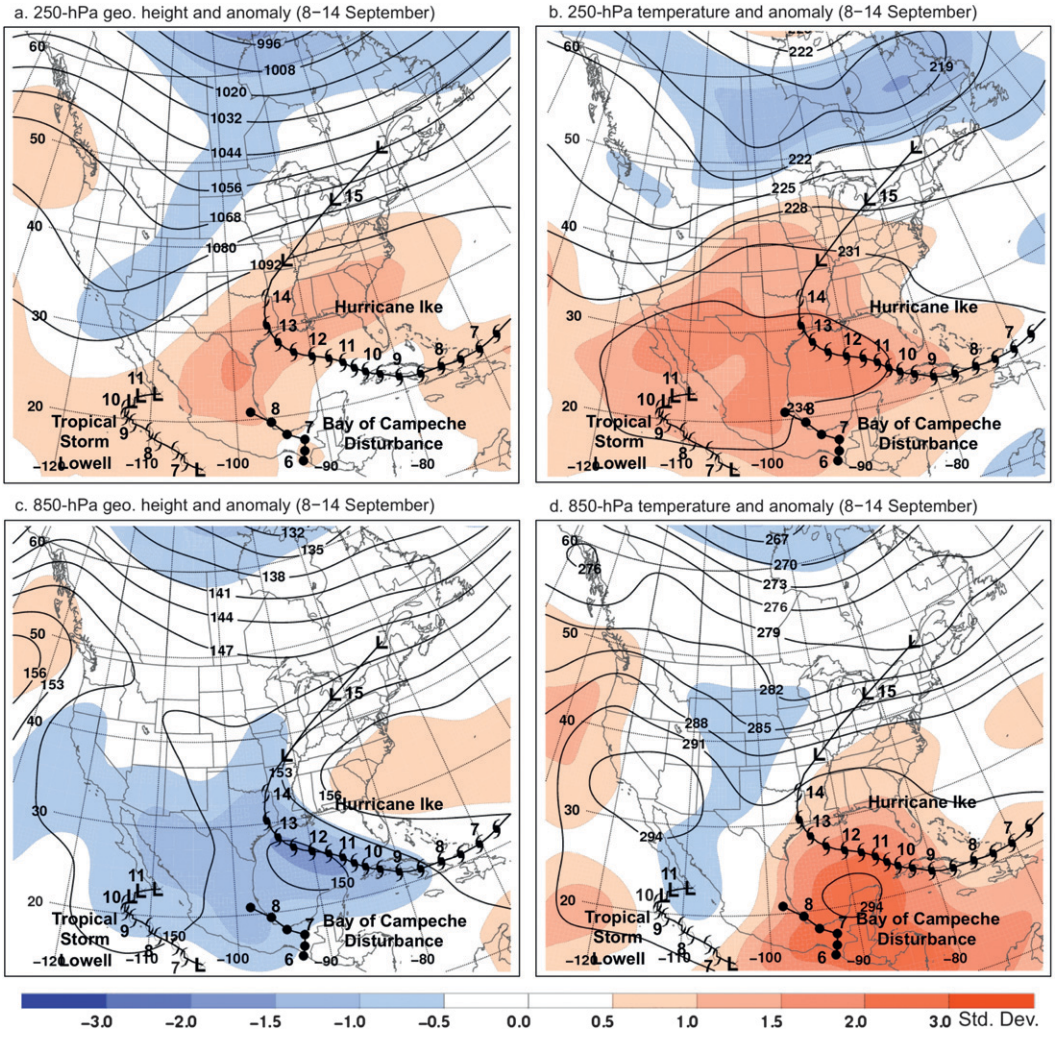

FIG. 2. The 250-hPa mean (a) geopotential height (solid contours every 12 dam) and (b) temperature (solid contours every 3 K) with respective standardized anomalies (shaded according to scale) for 8–14 Sep 2008. (c),(d) As in (a),(b), but for 850 hPa, respectively. Tracks of TC Ike, TC Lowell, and a disturbance over the Bay of Campeche are labeled at their 0000 and 1200 UTC positions (date indicated at 0000 UTC position) by symbols representing the intensity; standard hurricane, tropical storm, tropical depression (''L^x''), extratropical (''L''), and weak disturbance (filled circle) symbols are indicated.

''rainfall corridors'' (Fig. 3a). The western rainfall corridor marks the PRE development region over the Big Bend region of Texas. Rainfall that contributes to the western rainfall corridor is influenced in part by moisture from the stalled frontal boundary, the Bay of Campeche disturbance, and TC Lowell. The eastern rainfall corridor marks the landfall location of TC Ike over southeastern Texas and rainfall that contributes to the eastern rainfall corridor is influenced primarily by moisture from TC Ike. These two rainfall corridors merge over Missouri and extend toward the lower Great Lakes. The individual daily rainfall maps show a pronounced western rainfall corridor during 11–13 September that reflects daily accumulated precipitation associated with the three PREs (Figs. 3b–d) and a prominent merged rainfall corridor during 13–15 September that reflects the daily accumulated precipitation associated with PRE 3 and TC Ike (Figs. 3d–f).

c. *Moisture sources and transport*

The large-scale flow evolution prior to the development of the three PREs between 0000 UTC 6 September and 1200 UTC 10 September illustrates a favorable environment for the poleward transport of tropical moisture (Fig. 4). An axis of high PW values (>50 mm) that extends from near the southern tip of Texas to Mississippi and Tennessee associated with a cold front and an accompanying 250-hPa trough crossing the central plains at

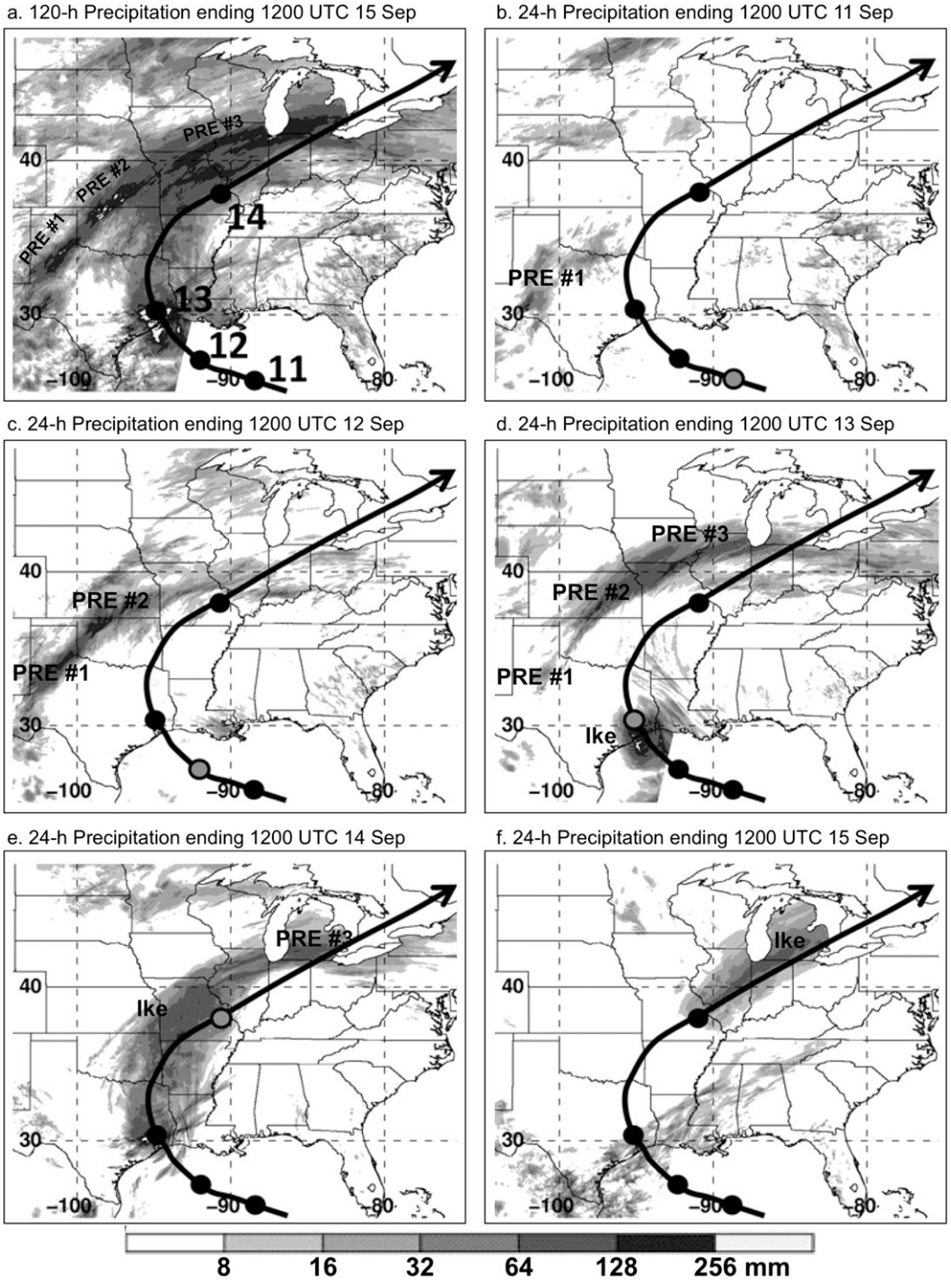

FIG. 3. Total accumulated precipitation (shaded in mm) from the NPVU QPE analyses for the (a) 120-h period ending 1200 UTC 15 Sep 2008, and the 24-h period ending 1200 UTC (b) 11, (c) 12, (d) 13, (e) 14, and (f) 15 Sep 2008. The track of TC Ike is labeled with black dots at the 1200 UTC positions. The gray dots in (b)–(f) mark the position of Ike at the analysis time indicated. The approximate locations of precipitation associated with the three PREs are labeled.

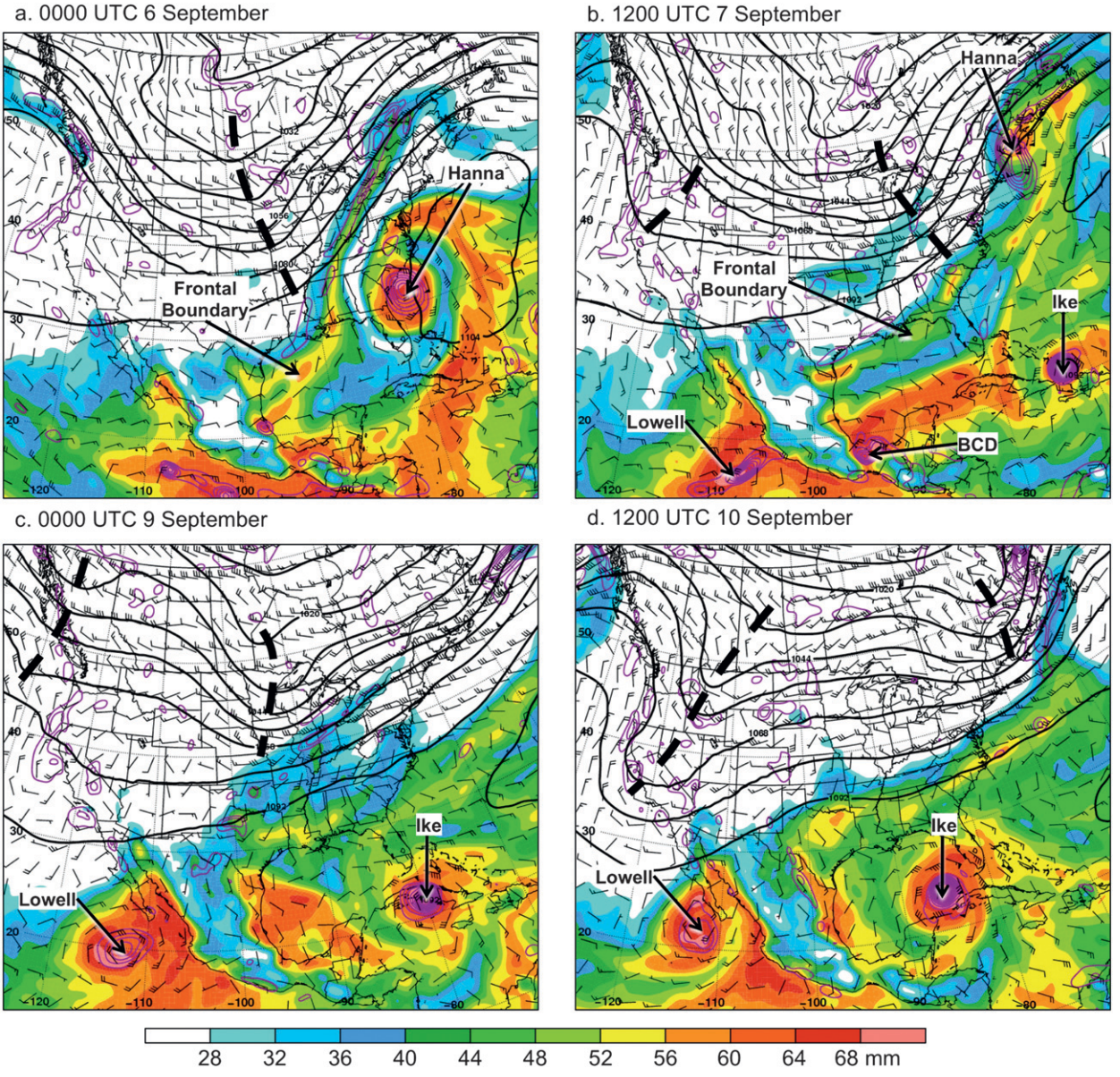

FIG. 4. The 250-hPa geopotential height (solid black contours every 12 dam), 700-hPa wind (pennant, full barb, and half barb denote 25.0, 5.0, and 2.5 m s^{-1}, respectively), 925–850-hPa relative vorticity (solid magenta contours every 5.0×10^{-5} s^{-1} starting at 5.0×10^{-5} s^{-1}), and PW (shaded in mm) at (a) 0000 UTC 6 Sep, (b) 1200 UTC 7 Sep, (c) 0000 UTC 9 Sep, and (d) 1200 UTC 10 Sep 2008. The TCs Hanna, Lowell, and Ike are labeled. The Bay of Campeche disturbance is labeled as "BCD." Thick dashed black lines indicate the 250-hPa trough axes.

0000 UTC 6 September is the initial moisture source for rainfall in west-central Texas (Fig. 4a). This 250-hPa trough approaches the Ohio Valley and lifts to the east-northeast as the cold front boundary stalls between southern Texas and South Carolina along the Gulf Coast by 1200 UTC 7 September (Fig. 4b).

At 1200 UTC 7 September, a 700-hPa cyclonic circulation center is located over the southern Gulf of Mexico and Bay of Campeche. The corresponding 925–850-hPa cyclonic vorticity maximum, located within the second moisture source over the Bay of Campeche (PW values >60 mm; Fig. 4b), evolves from the consolidation of disparate vorticity maxima over the Isthmus of Tehuantepec (not shown). Southeasterly lower-tropospheric flow poleward of the Bay of Campeche disturbance facilitates the transport of tropical moisture toward the northeast coast of Mexico (Fig. 4b). The moisture associated with the stalled frontal boundary and the Bay of Campeche disturbance

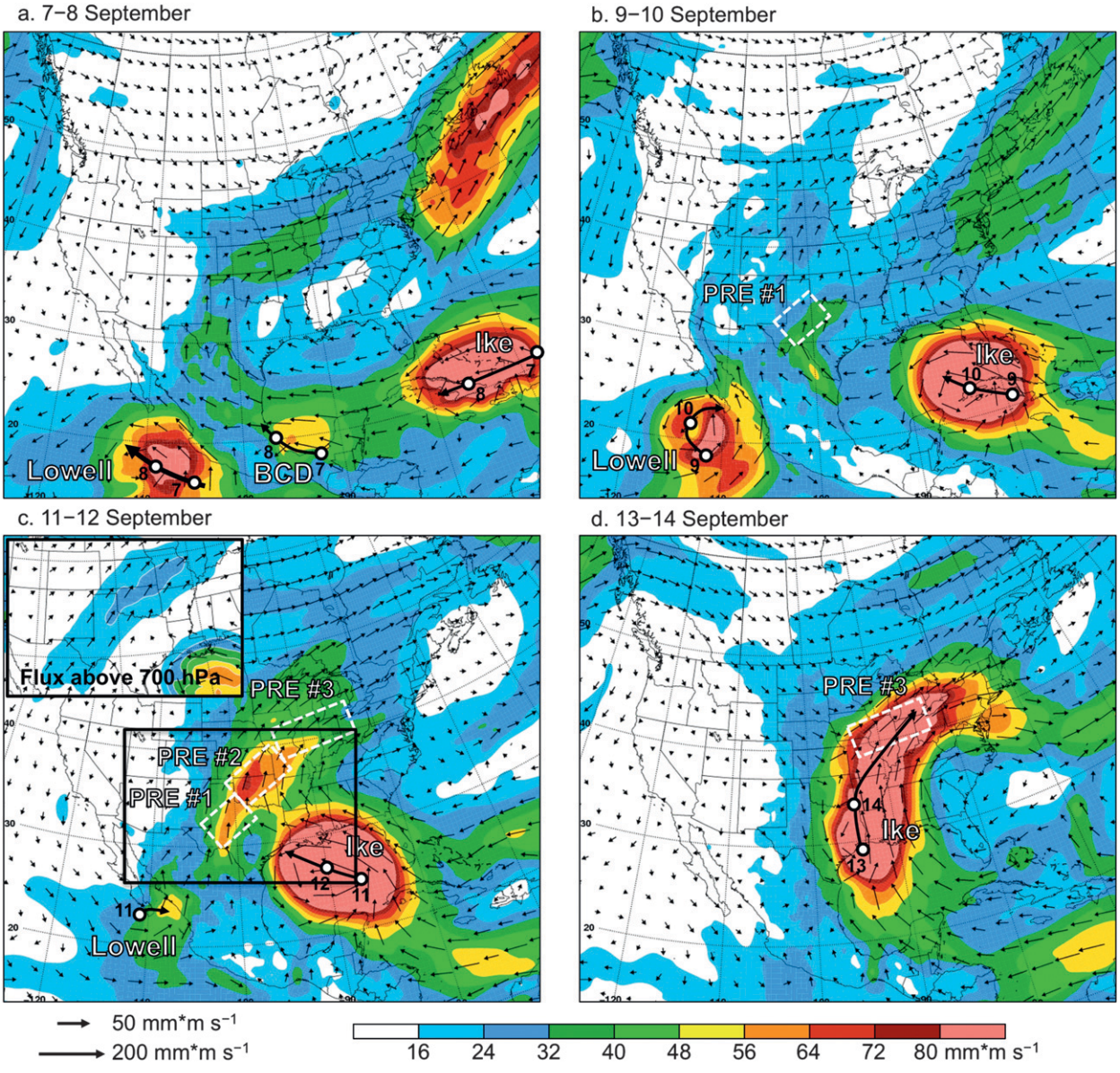

FIG. 5. Two-day mean 1000–100-hPa PW flux (shaded and vectors in mm m s^{-1}) for (a) 7–8, (b) 9–10, (c) 11–12, and (d) 13–14 Sep 2008. PW flux calculated for 700–100-hPa is inset in (c). Two-day tracks are shown for each TC Lowell, TC Ike, and the Bay of Campeche disturbance.

remains separated by a region of drier air (PW values <40 mm) over the Gulf of Mexico. The third moisture source that is associated with PRE development and maturation is represented by a plume of moist air (PW values >48 mm) located between the west coast of Mexico and TC Lowell over the eastern North Pacific on 7–9 September (Figs. 4b,c). The fourth tropical moisture source that influences PRE development and maturation is represented by moist air (PW values >50 mm) associated with TC Ike over the eastern Gulf of Mexico at 1200 UTC 10 September (Fig. 4d).

Two-day mean vertically integrated moisture (PW) fluxes, calculated following the methodology of Neiman et al. (2008) and via Eq. (1) of Moore et al. (2012), depict the moisture transport critical to multiple PRE development (Fig. 5). The PW flux for 7–8 September illustrates moisture transport from three of the aforementioned lower-latitude source regions associated with TC Lowell over the eastern Pacific, the disturbance over the Bay of Campeche, and TC Ike over eastern Cuba (Fig. 5a). The PW flux maximum located over the Rio Grande Valley and central Texas for 9–10 September represents the

poleward transport of the Bay of Campeche moisture up the Rio Grande Valley and a merger of this high PW air with the stalled frontal boundary over east Texas along the Texas–Oklahoma border (Fig. 5b). The amalgamation of these two moisture sources provides a favorable environment for the organization of rainfall over west-central Texas on 10 September.

On 10 September, high PW air associated with TC Lowell approaches the southern tip of the Baja of California in southwesterly flow ahead of a deep 250-hPa trough over the western United States (Fig. 4d). By 11–12 September, a PW flux maximum develops across the Mexican Plateau and extends northeastward over the central plains (Fig. 5c). Moisture transport across the Mexican Plateau is emphasized by integrated PW fluxes calculated for 700–100 hPa shown inset in Fig. 5c. The PW flux maximum over the central plains on 11–12 September represents a merger between moisture associated with TC Lowell, moisture associated with the Bay of Campeche disturbance, and moisture associated with the stalled frontal boundary. The amalgamation of these three moisture sources, which now includes a TC moisture source region, provides a favorable environment for the development of PRE 1 late on 10 September and the development of PRE 2 on 11–12 September.

The initial development of PRE 3 occurs in associated with the northeastward transport of moisture represented by the central plains PW flux maximum over Missouri and Illinois on 11–12 September (Fig. 5c). The poleward PW flux maximum associated with TC Ike over the northern Gulf of Mexico coast eventually merges with the central plains flux maximum by 13–14 September and further influences the evolution and maturation of PRE 3 (Fig. 5d).

d. Satellite perspective

Select satellite infrared (IR) imagery for 9–13 September complements the precipitation and PW analyses presented in sections 3a–c (Fig. 6). At 1245 UTC 9 September, regions of deep convection (illustrated by clusters of high, cold cloud tops) are evident along the west coast of Mexico ahead of TC Lowell, along the northeastern coast of Mexico collocated with the Bay of Campeche disturbance, and over Cuba in conjunction with TC Ike (Fig. 6a). These regions of deep convection are located within the regions of high PW air observed in previous PW analyses (e.g., Fig. 4c). The extent of deep convection and associated cloud cover between TC Lowell and the central plains is consistent with the northeastward transport of upper-tropospheric moisture toward the maturation region of PRE 1 over Texas by 1800 UTC 11 September (Fig. 6b), toward the development region of PRE 2 over Kansas by 1200 UTC 12 September (Fig. 6c), and toward the region where PRE 2 and PRE 3 merged over Kansas, Missouri, Nebraska, and Iowa by 0915 UTC 13 September (Fig. 6d). As TC Ike makes landfall shortly before 0915 UTC 13 September, the deep convection surrounding the storm remains separate from PRE 3 between eastern Iowa and lower Michigan (Fig. 6d) while the PW flux maxima associated with TC Lowell, the Bay of Campeche disturbance, the stalled frontal boundary, and TC Ike are in the process of merging on 13 September (Fig. 5d).

e. Lagrangian trajectory analysis

Backward trajectories computed for a 72-h period ending at representative times and ending on isobaric levels between 925 and 200 hPa over Midland (MAF), Texas; Amarillo (AMA), Texas; Des Moines (DSM), Iowa; Rockford (RFD), Illinois; Benton Harbor (BEH), Michigan; and Springfield (SGF), Missouri, show the transport of moisture from the four moisture source regions toward the three PREs and the presence of warm-air advection (i.e., trajectory paths veering with height) during the development and maturation of the three PREs (Fig. 7).

The trajectory analysis confirms that the maturation of PRE 1 near MAF at 1800 UTC 10 September (Fig. 7a) and the development of PRE 2 near AMA at 0000 UTC 12 September (Fig. 7b) are associated with lower-tropospheric air parcels that originate over the western Gulf of Mexico in the vicinity of the stalled frontal boundary and the Bay of Campeche, and upper-tropospheric air parcels that originate over the eastern North Pacific in the vicinity of TC Lowell. Additionally, the air parcel arriving at MAF at 1800 UTC 10 September with a near-surface (925 hPa) source region over northern plains is indicative of weak upslope flow in a shallow cool air mass that is situated beneath air parcels that arrive at MAF along clockwise-turning paths from the southern through the Southwest with height, evidence of warm-air advection, above the shallow cool air mass.

The maturation of PRE 3 near DSM, RFD, and BEH (Figs. 7c–e, respectively) on 13 September is associated with a transition in lower-tropospheric air parcel source regions from coastal Texas in the vicinity of the stalled frontal boundary to the Caribbean and Bahamas in the vicinity of TC Ike, and a persistent upper-tropospheric air parcel source region over the eastern North Pacific and Mexico in the vicinity of TC Lowell. Air parcel trajectory paths that veer with height as they reach DSM, RFD, and BEH, respectively, are consistent with extended warm-air advection and abrupt deep ascent as they reach these locations (Figs. 7c–e). The merger of TC Ike and PRE 3 near SGF at 0600 UTC 14 September is associated with lower-tropospheric air parcel source regions over the tropical boundary layer ahead of TC Ike over Cuba (Fig. 7f), and upper-tropospheric air parcel source regions

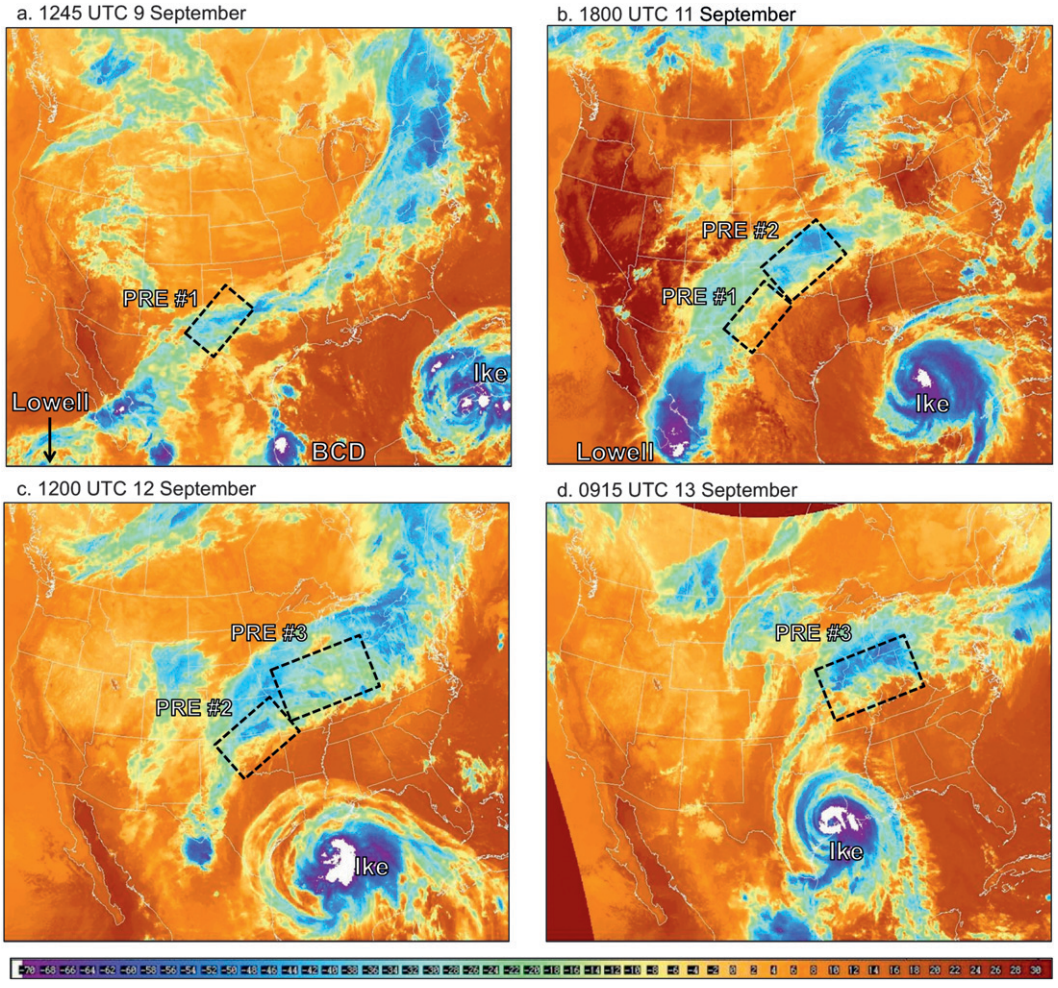

FIG. 6. *Geostationary Operational Environmental Satellite (GOES)-12* enhanced infrared satellite imagery (shaded according to the color bar in °C) at (a) 1245 UTC 9 Sep, (b) 1800 UTC 11 Sep, (c) 1200 UTC 12 Sep, and (d) 0915 UTC 13 Sep 2008.

over the southwest Gulf of Mexico that spiral cyclonically and ascend within the circulation around TC Ike over eastern Texas.

4. Results: PRE organization

a. Organization of PRE 1

The development of PRE 1 is influenced by the evolution of two surface troughs extending 1) along the Gulf Coast through central Texas as a frontal trough (the stalled frontal boundary) at 1200 UTC 7 September and 2) poleward from the Bay of Campeche disturbance along the Mexican coast as an inverted trough at 1200 UTC 7 September (Fig. 8a). The Gulf Coast frontal trough is associated with weak lower-tropospheric easterly geostrophic flow (upslope in western Texas) at 1200 UTC 7 September (Fig. 8a), which is subsequently enhanced by anticyclogenesis over the northern plains by 1200 UTC 8 September (Fig. 8b). The inverted trough along the Mexican coast is associated with weak southeasterly geostrophic flow over the western Gulf of Mexico, eastern Mexico, and the lower Rio Grande Valley at 1200 UTC 7 September, which is subsequently enhanced by the poleward extension of this trough toward southern Texas by 1200 UTC 8 September (Figs. 4b,c and 8a,b). The combined enhanced easterly geostrophic flow over the central plains and the enhanced southeasterly geostrophic flow over the lower Rio Grande Valley helps to transport moisture from the stalled frontal boundary and Bay of Campeche disturbance, respectively, toward to the development region of PRE 1 over western Texas.

Anticyclogenesis over the central plains between 1200 UTC 7 September and 1200 UTC 8 September results in a terrain-influenced equatorward surge of cooler air east of the Rockies (Fig. 8b). The surge of cooler air further enhances the easterly (upslope) flow over the Oklahoma

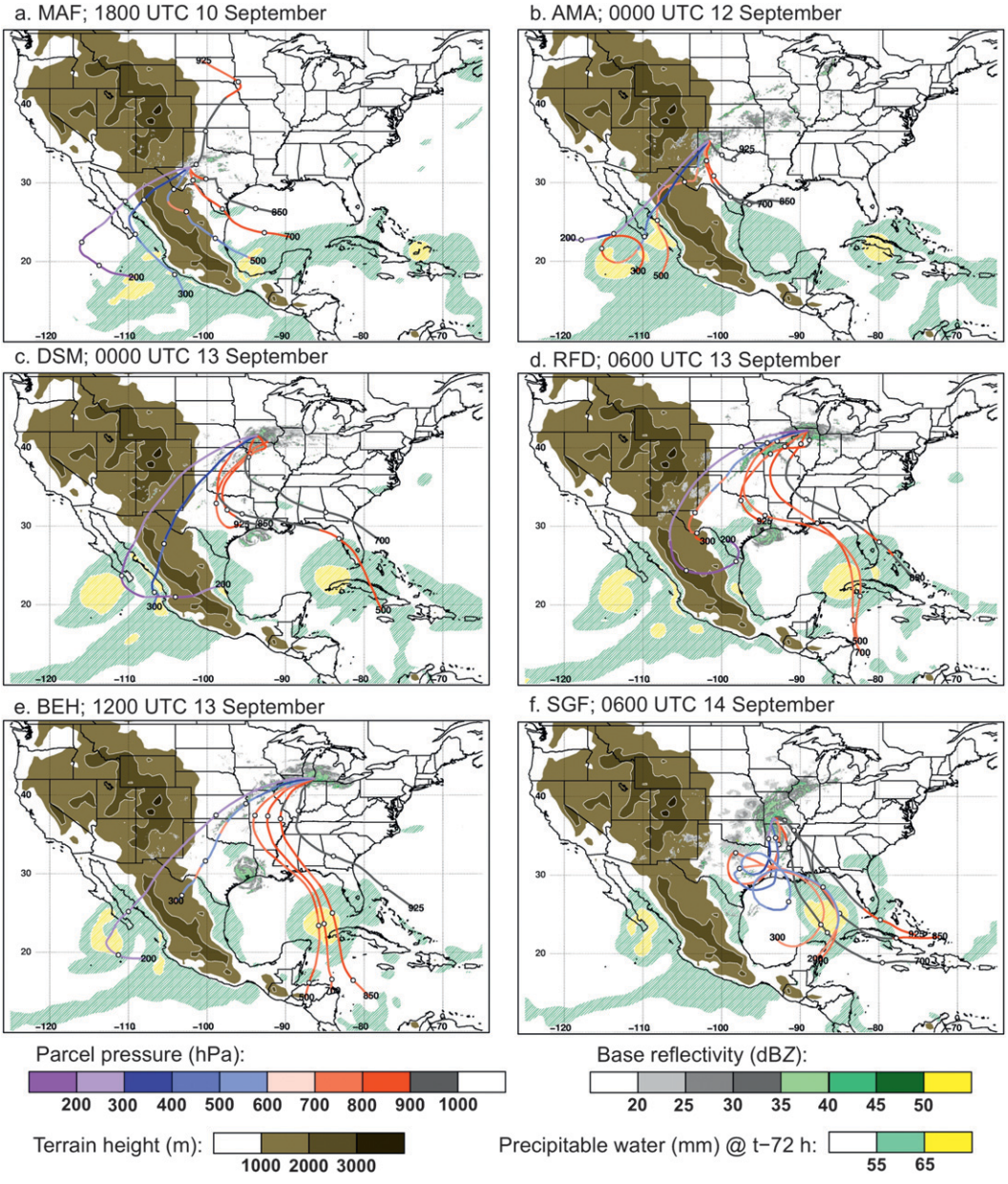

FIG. 7. The 72-h backward air parcel trajectories with endpoints at (a) MAF at 1800 UTC 10 Sep, (b) AMA at 0000 UTC 12 Sep, (c) DSM at 0000 UTC 13 Sep, (d) RFD at 0600 UTC 13 Sep, (e) BEH at 1200 UTC 13 Sep, and (f) SGF at 0600 UTC 14 Sep 2008. Air parcel pressure following trajectories is shaded in hPa according to purple-blue-red color bar. PW values are shaded in green and yellow above 55 and 65 mm, respectively, 72 h prior to trajectory termination (i.e., at air parcel origination). Base radar reflectivity values are shaded according to the gray–green color bar at the time of trajectory termination. Terrain height is shaded every 1000 m above 1000 m according to the brown color bar.

and Texas Panhandles southward into southern and western Texas by 1200 UTC 9 September (Fig. 8c). The evolution of the 1000–500-hPa thickness field relative to the corridor of 250-hPa westerly winds >30 m s^{-1} (i.e., a weak STJ) shows that the leading edge of this cool surge crosses the axis of the STJ in the 24 h ending at 1200 UTC 9 September. Upslope easterly flow over parts of Texas, New Mexico, and northern Mexico near the leading edge of this surge (see also the northerly 925-hPa trajectory in Fig. 7a) represents a region of weak warm-air advection beneath the equatorward entrance region of the STJ. The juxtaposition of these dynamical features provides conditions favorable for quasigeostrophic (QG) forcing for ascent (not shown) during the organization of rainfall over west Texas prior to the development of PRE 1 after 0600 UTC 10 September.

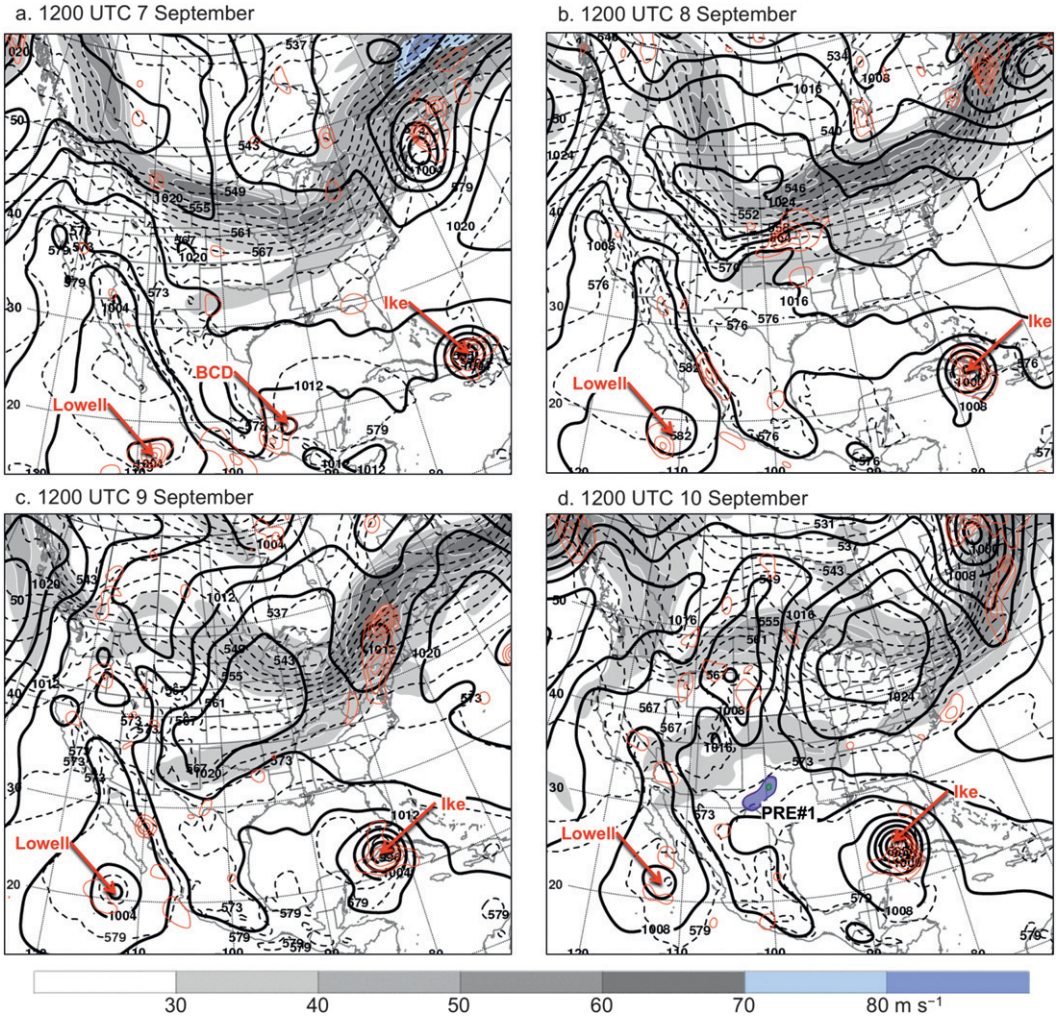

FIG. 8. Sea level pressure (solid black contours every 4 hPa), 1000–500-hPa thickness (dashed black contours every 3 dam), 250-hPa wind speed (shaded according to the color bar and thin solid white contours every 10 m s^{-1}), and 700-hPa ascent (solid red contours every 2.0×10^{-3} hPa s^{-1} starting at -2.0×10^{-3} hPa s^{-1}) at 1200 UTC (a) 7, (b) 8, (c) 9, and (d) 10 Sep 2008. Regions of 700-hPa ascent associated with individual PREs are shaded and indicated.

b. Organization of PRE 2

The development of PRE 2 is influenced by the eastward displacement of the central plains anticyclone, lee trough development, and enhanced southerly lower-tropospheric geostrophic flow over the Texas Panhandle northeastward toward Canada between 1200 UTC 10 September and 1200 UTC 11 September (Figs. 8d and 9a). This increased southerly flow is consistent with moisture transport up the Rio Grande Valley from the Bay of Campeche to the southern and central plains toward the development region of PRE 2 over Oklahoma and Kansas (Figs. 4d and 5b).

The development of PRE 2 is also influenced by an increase in southerly lower-tropospheric flow ahead of TC Lowell, which increases the transport of moisture toward northwestern Mexico, the Sierra Madre Occidental Mountains, and the southern plains beneath the equatorward entrance region of the STJ at 1200 UTC 11 September (Figs. 5c and 9a). The increased southerly flow influences orographic ascent and deep convection over western Mexico (Fig. 6b). The 1000–500-hPa thickness values simultaneously increase over Mexico and Texas as the STJ intensifies from ~30 to >40 m s^{-1} over northwest Mexico, Arizona, and New Mexico between 1200 UTC 10 September and 1200 UTC 11 September (Figs. 8d and 9a). The intensification of the STJ occurs in conjunction with the deep convection proximate TC Lowell and the development of PRE 1 (Figs. 6a,b). Diabatic heating associated with these regions of deep convection likely favored an increase in the meridional 1000–500-hPa thickness gradient and likely influenced the intensification

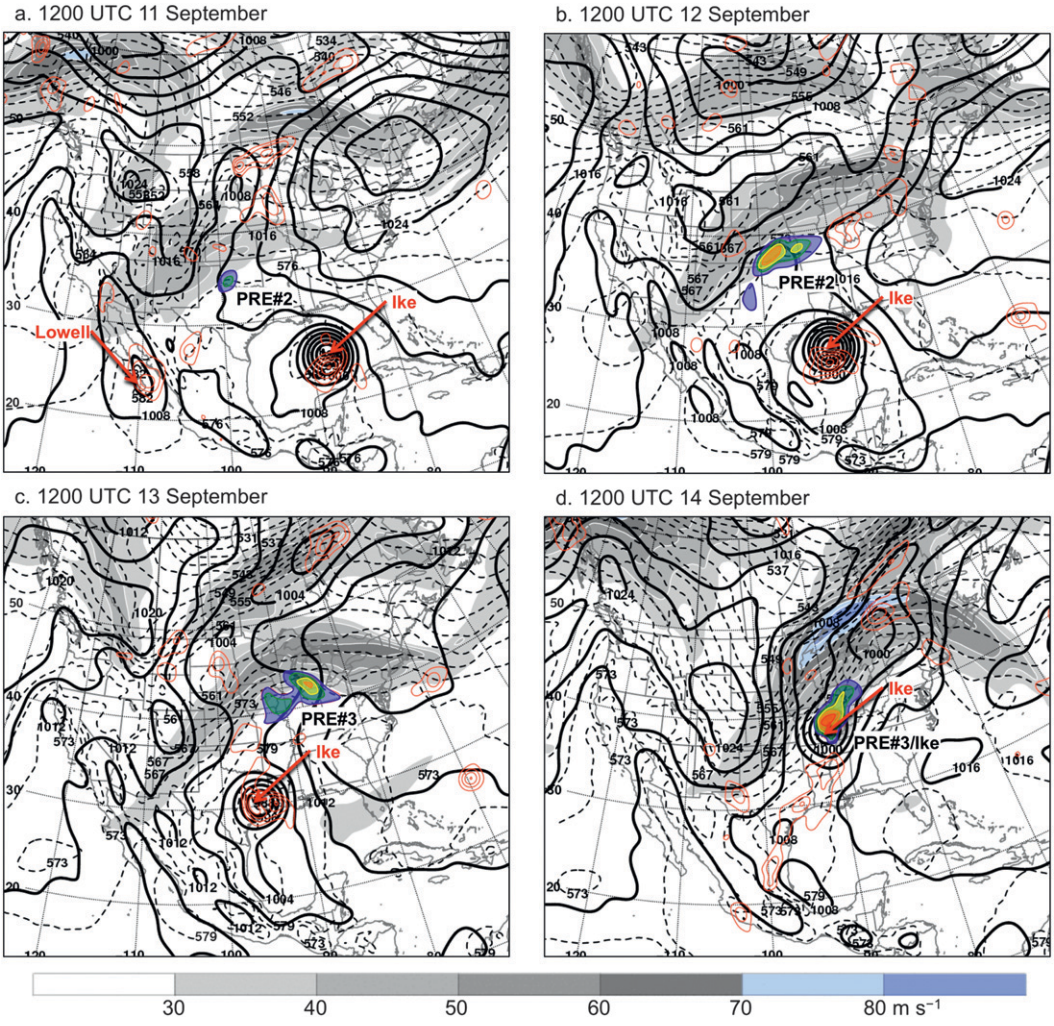

FIG. 9. As in Fig. 8, but for 1200 UTC (a) 11, (b) 12, (c) 13, and (d) 14 Sep 2008.

of STJ. In turn, the intensification of the STJ helped to maintain the favorable location for QG forcing for ascent (not shown) over the development region of PRE 2.

c. *Organization of PRE 3*

The initial development of PRE 3 is influenced by a weak inverted trough over Oklahoma along the warm side of a baroclinic zone that extends northeastward from New Mexico to the western Great Lakes at 1200 UTC 12 September (Fig. 9b). Comparison of Figs. 1a, 3c, and 9a,b also shows that PRE 2 develops along this inverted trough over Oklahoma. Weak inferred warm-air advection over eastern Kansas and Missouri along the inverted trough at 1200 UTC 12 September contributes to the ascent over Oklahoma, Kansas, and Missouri that helps to sustain heavy rainfall associated with PRE 2 and the initial development of PRE 3 (Figs. 6c and 9b). The STJ continues to intensify from ~40 m s^{-1} over Colorado and New Mexico at 1200 UTC 11 September to >60 m s^{-1} over the Great Lakes region by 1200 UTC 12 September (Figs. 9a,b). The intensification the STJ is consistent with an increase in the meridional 1000–500-hPa thickness gradient due to the combined effects of lower-tropospheric cold-air advection over the western Great Lakes behind a weak disturbance that moved from extreme western Minnesota at 1200 UTC 11 September (Fig. 9a) to northern Lake Huron 24 h later (Fig. 9b), lower-tropospheric warm-air advection in the equatorward entrance region of the STJ, and likely diabatic heating over Kansas and Oklahoma in association with PREs 2 and 3 (Figs. 6c and 9b). The intensification of the STJ maintained a favorable region of QG forcing for ascent over the central plains (not shown).

The development of PRE 3 is further influenced by the evolution of an inverted warm frontal trough poleward

of TC Ike over the Great Lakes region by 1200 UTC 13 September (Fig. 9c). Warm-air advection intensifies to the east of this warm frontal trough along which PRE 3 becomes more organized (Figs. 6d and 9c). The STJ observed over the Great Lakes region 24 h earlier (Fig. 9b) begins to zonally elongate as the western portion of the STJ ''back builds'' across the northern plains and the eastern portion of the STJ shifts eastward over the Northeast between 1200 UTC 13 September and 1200 UTC 14 September (Figs. 9c,d). The warm frontal trough and PRE 3 are located in the equatorward entrance region of the back-building portion of the STJ (Fig. 9c), which suggests the development of PRE 3 may have involved a synergistic relationship between precipitation processes along the warm frontal trough and within the equatorward entrance region of the STJ. A weak surface cyclone located northeast of Lake Huron at 1200 UTC 14 September develops along the PRE 3 warm frontal trough 24 h earlier (Figs. 9c,d). Northerly flow in the wake of this cyclone strengthens the lower-tropospheric baroclinic zone ahead of TC Ike (Fig. 9d).

5. Results: PRE structure and evolution

a. Structure and evolution of PRE 1

The merger of moisture from the stalled frontal boundary and the Bay of Campeche disturbance in the development region of PRE 1 is evident in the 0000 and 0600 UTC 9 September soundings from Del Rio (DRT), Texas, as PW values increase from 35 to 50 mm [Fig. 10b (sounding locations given in Fig. 10a)], and subsequently to 62 mm by 1200 UTC 10 September (not shown). The merger of these two moisture sources contributes to the organization of rainfall prior to the development of PRE 1 after 0000 UTC 10 September in association with the consolidation of weak scattered shower activity in upslope flow over western Texas. PRE 1 reaches maturity over western and north-central Texas and southern Oklahoma along a weak baroclinic zone sustained by terrain-channeled lower-tropospheric northerly flow beneath deeper southerly flow aloft (Figs. 7a and 8d) at 1800 UTC 10 September as shown by composite base reflectivity (Fig. 11a), and the onset of heavy precipitation in the Midland (MAF), Texas, meteogram [Fig. 12b (meteogram locations given in Fig. 12a)]. The arrival of moisture from TC Lowell in the middle and upper troposphere in deep west-southwesterly flow into the environment of mature PRE 1 is evident from a comparison of the aforementioned DRT soundings (Fig. 10b) and MAF soundings for 1800 UTC 9 September and 0600 UTC 10 September (Fig. 10c). PRE 1 dissipates over Oklahoma by 0600 UTC 11 September (not shown).

b. Structure and evolution PRE 2

The merger of moisture from the stalled frontal boundary, the Bay of Campeche disturbance, and TC Lowell in the development region of PRE 2 is evident in the 1800 UTC 10 September and 0000 UTC 12 September soundings from Lamont (LMN), Oklahoma, with PW values increasing from 35 to 55 mm (Fig. 10d). Evidence for the arrival of moisture from TC Lowell is given by the increase in the observed tropospheric wet bulb potential temperature above ~700 hPa to ~23°C at LMN at 0000 UTC 12 September, a value characteristic of a moist tropical boundary layer (Fig. 10d). The merger of these three moisture sources is associated with a region of weak precipitation that develops over the Big Bend region of Texas at 0000 UTC 11 September (not shown) and organizes into PRE 2 over Oklahoma and southeast Kansas by 1800 UTC 11 September (Fig. 11b). Although convective precipitation rates during the development of PRE 2 likely contributed to the daily record rainfall at LBB on 11 September (Fig. 12c), PRE 2 is primarily associated with stratiform precipitation over Oklahoma as evidenced by relatively low CAPE values (50–300 J kg^{-1}) at LMN (Fig. 10d), composite base reflectivity values of 20–40 dBZ (Fig. 11b), precipitation rates $<$10 mm day^{-1} shown in a meteogram at Clinton–Sherman (CSM), Oklahoma, on 11 September (Figs. 12d), and deep warm-air advection accompanying the observed precipitation observed in the profiler time series from LMN (Fig. 13a).

c. Structure and evolution of PRE 3

PRE 3 organizes prior to the maturity of PRE 2 and is represented by scattered reflectivity regions over southeastern New Mexico at 1800 UTC 11 September (Fig. 11b). The poleward transport of moisture over the southern plains during the development of PRE 3 coincides with lower- and midtropospheric warm-air advection above a strengthening LLJ as illustrated by a profiler time series from Neodesha (NDS), Kansas, on 12 September (Fig. 13b). By 0600 UTC 12 September, PRE 3 extends from western Texas (associated with newly organized precipitation) to Illinois (associated with the remnants of PRE 2; Fig. 11c). The northeastward transport of moisture from Oklahoma to Kansas that sustains the northeast portion of PRE 3 (formerly PRE 2) is evident in the 0000 UTC 13 September sounding from Topeka (TOP), Kansas, as PW values increase to 57 mm (Fig. 10e). A meteogram for ICT suggests that sustained moderate-to-heavy rain accompanies the development of PRE 3 as it evolves over Kansas at 1200 UTC 12 September (Fig. 12e).

At 0900 UTC 13 September, mature PRE 3 appears as a broad anticyclonically curved band of heavy rain that extends from eastern Kansas northeastward across

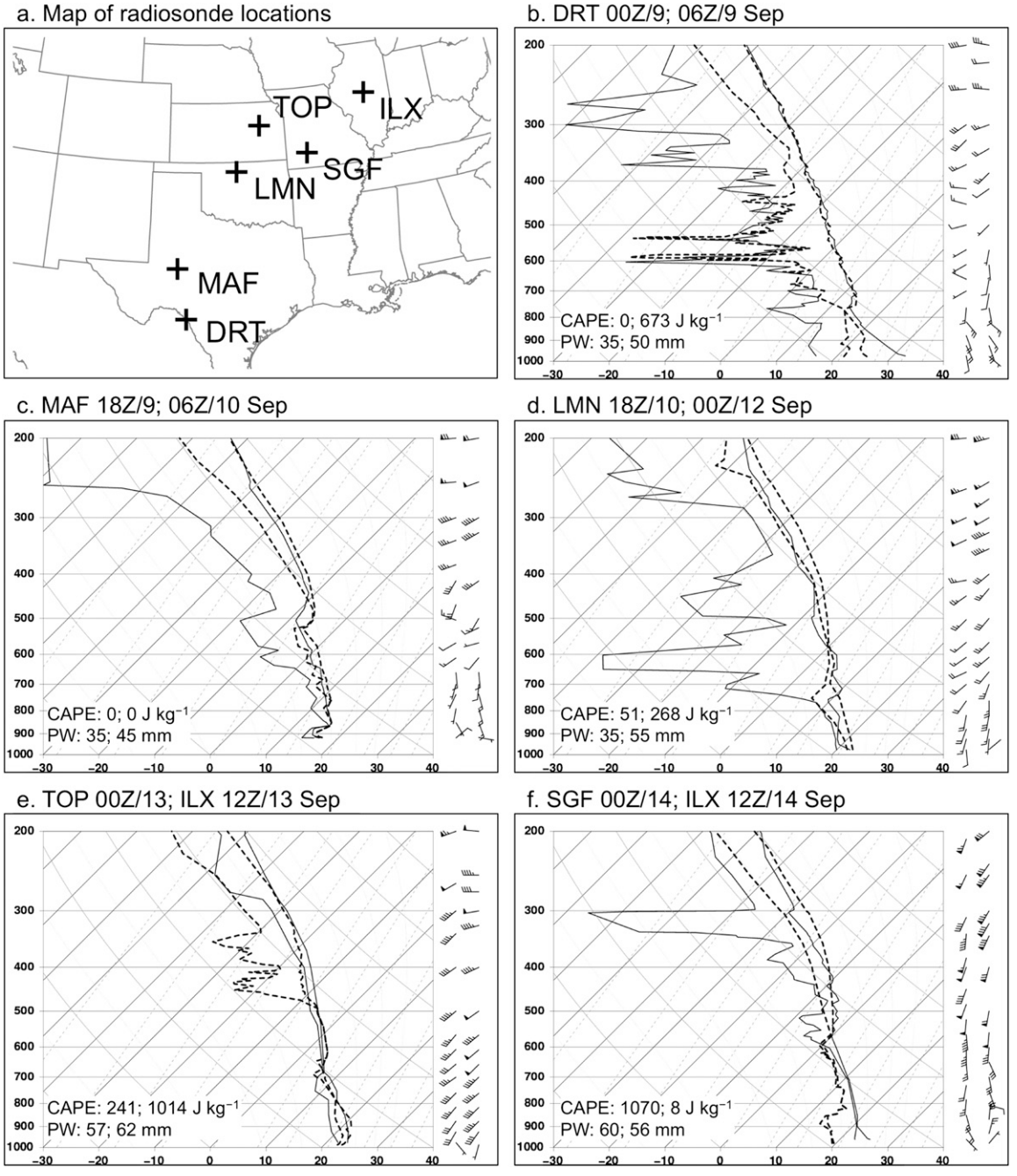

FIG. 10. (a) Radiosonde locations for skew T-log$p$ diagram of temperature (°C), dewpoint (°C), and wind (pennant, full barb, and half barb denote 25.0, 5.0, and 2.5 m s^{-1}, respectively). (b) DRT at 0000 (solid; left wind barbs) and 0600 (dashed; right wind barbs) UTC 9 Sep, (c) MAF at 1800 UTC 9 Sep (solid; left wind barbs) and 0600 UTC 10 Sep (dashed; right wind barbs), (d) LMN at 1800 UTC 10 Sep (solid; left wind barbs) and 0000 UTC 12 Sep (dashed; right wind barbs), (e) TOP at 0000 UTC 13 Sep (solid; left wind barbs) and ILX at 1200 UTC 13 Sep (dashed; right wind barbs), and (f) SGF at 0000 UTC 14 Sep (solid; left wind barbs) and ILX at 1200 UTC 14 Sep 2008 (dashed; right wind barbs). The PW (mm) and CAPE (J kg^{-1}) values are indicated in (b)–(f).

northern Illinois and eastward into northwestern Ohio (Fig. 11d). At this time, PRE 3 is clearly distinct from the TC Ike rain shield located over southeast Texas. The maturation of PRE 3 occurs as moisture from TC Ike is transported poleward along a strong LLJ toward Illinois on 13 September (Fig. 5d) as evidenced by 20–25 m s^{-1} southwesterly flow in a profiler time series from Winchester (WNC), Illinois, on 13 September (Fig. 13c). A 1200 UTC 13 September sounding from Lincoln (ILX), Illinois, illustrates the arrival of moisture from TC Ike in

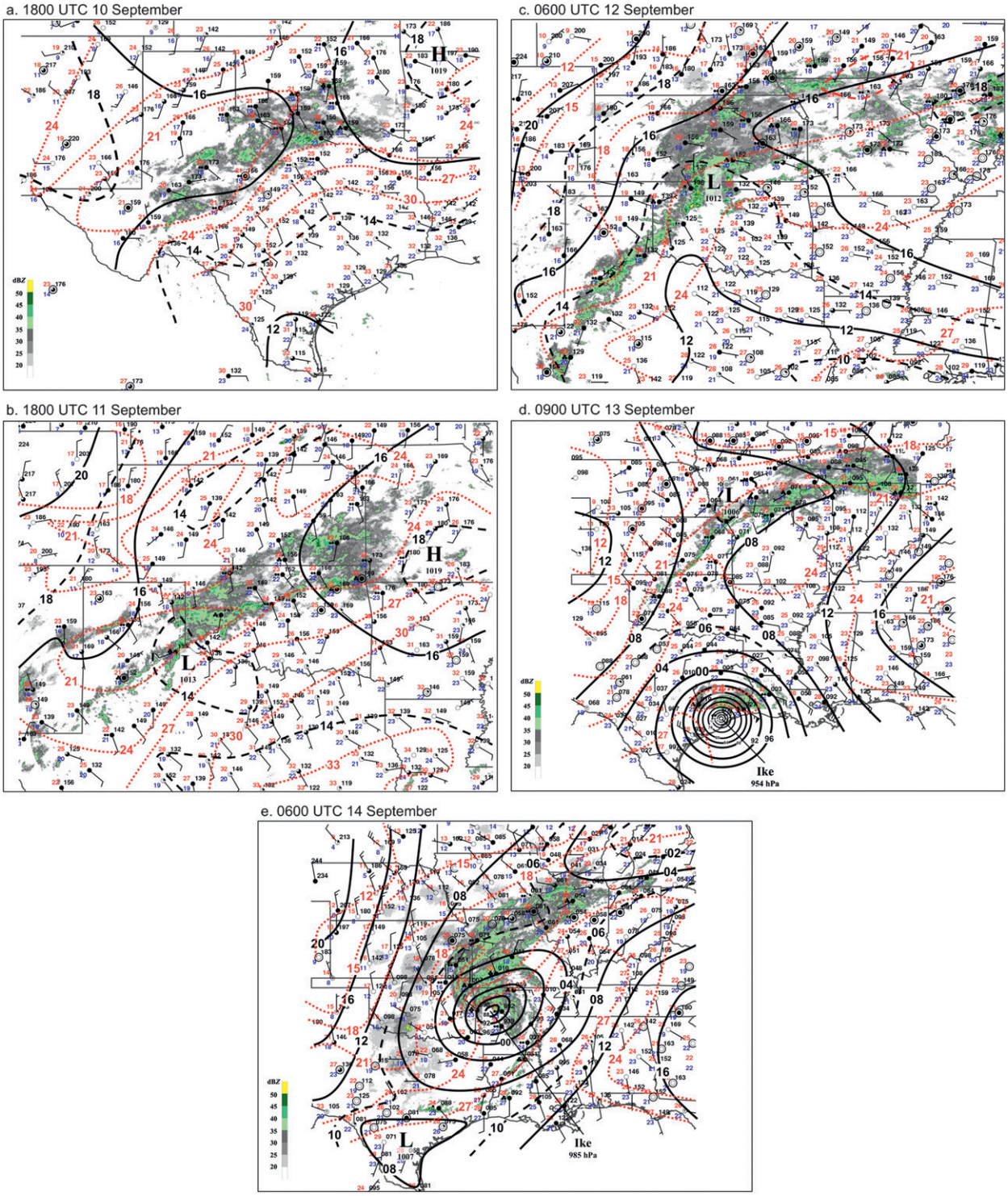

FIG. 11. Standard surface observations of temperature (°C), dewpoint temperature (°C), surface altimeter (hPa), present weather, cloud cover, and wind (pennant, full barb, and half barb denote 25.0, 5.0, and 2.5 m s^{-1}, respectively) overlaid on WSR-88D base reflectivity (shaded according to the color bar in dBZ). Surface temperature (dashed red contours every 2°C) and altimeter (solid black contours every 4 hPa, except dashed for emphasis every 2 hPa in some location) are contoured at (a) 1800 UTC 10 Sep, (b) 1800 UTC 11 Sep , (c) 0600 UTC 12 Sep, (d) 0900 UTC 13 Sep, and (e) 0600 UTC 14 Sep 2008.

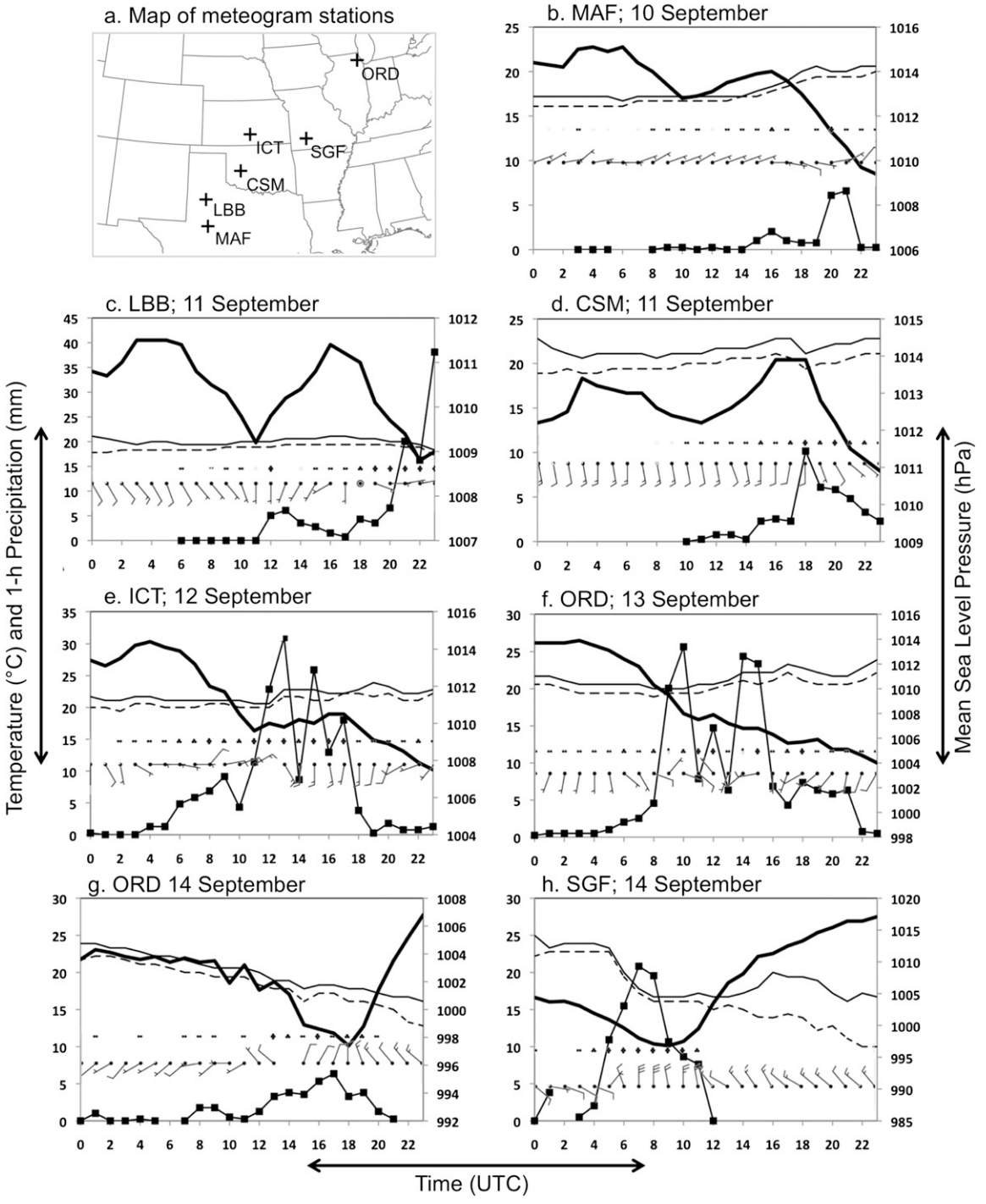

FIG. 12. Surface meteograms for locations given in (a) of sea level pressure (thick solid contour in hPa), temperature (thin solid contour in °C), dewpoint temperature (dashed contour in °C), 1-h total precipitation (thin solid contour with square markers in mm), present weather (symbols), sky cover (station model fill), and wind (pennant, full barb, and half barb denote 25.0, 5.0, and 2.5 m s^{-1}, respectively) for (b) MAF on 10 Sep, (c) LBB on 11 Sep, (d) CSM on 11 Sep, (e) ICT on 12 Sep, (f) ORD on 13 Sep, (g) ORD on 14 Sep, and (h) SGF on 14 Sep 2008.

association with PW values >60 mm (Fig. 10e). The warm, moist boundary layer with moderate CAPE values (1014 J kg^{-1}) at ILX supports heavy and likely convective rainfall within PRE 3 (Fig. 11d).

Heavy rainfall associated with PRE 3 occurs prior to, during, and immediately after the passage of a weak surface boundary near 1200 UTC 13 September at ORD as evidenced by a meteogram containing a gradual wind

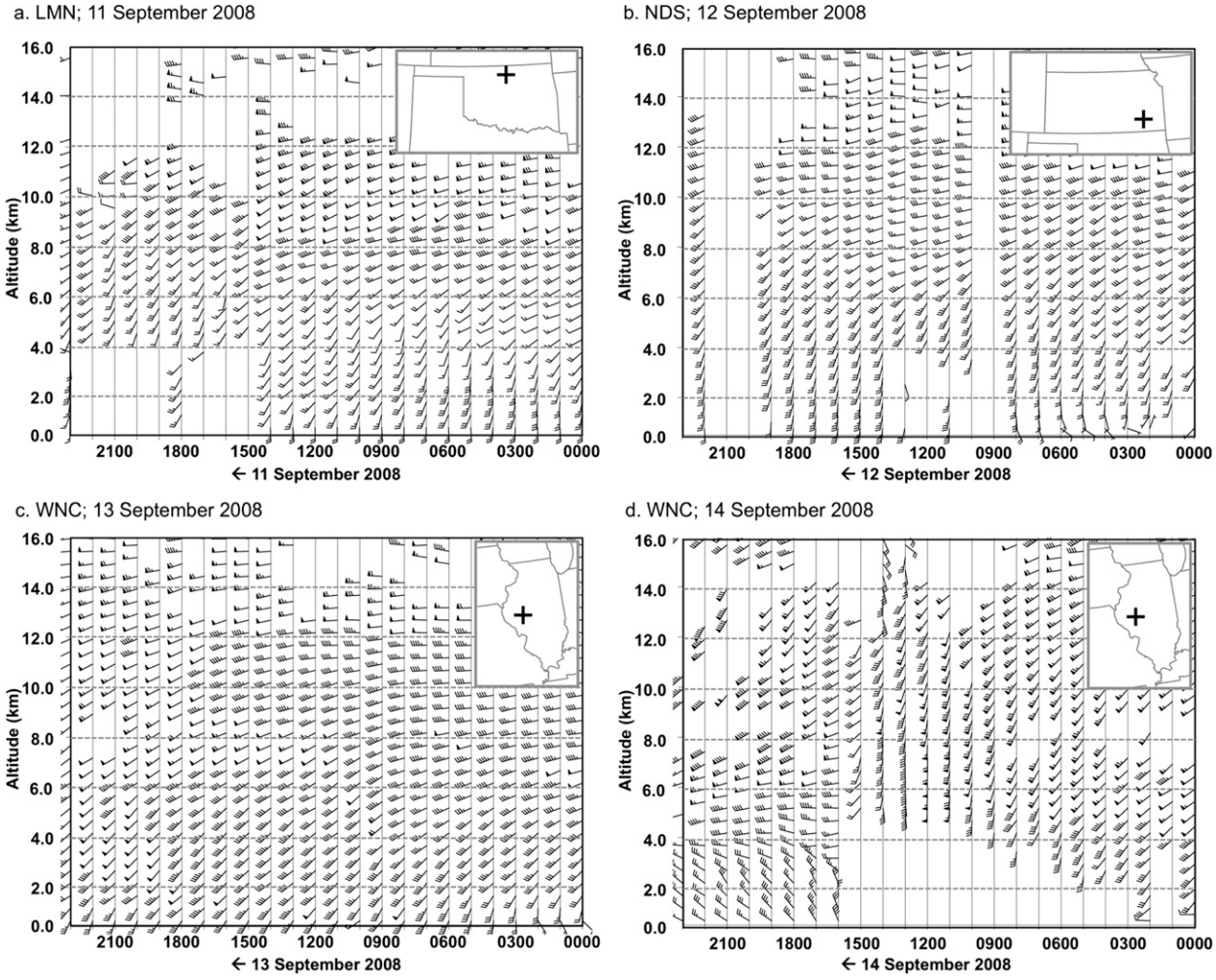

FIG. 13. Time (UTC)–height (km MSL) sections of NOAA profiler wind (pennant, full barb, and half barb denote 25.0, 5.0, and 2.5 m s^{-1}, respectively) observations for (a) LMN on 11 Sep, (b) NDS on 12 Sep, (c) WNC on 13 Sep, and (d) WNC on 14 Sep 2008.

shift from east-southeast to southwest (albeit with considerable directional variability; Fig. 12f). The sequence of precipitation intensity and wind direction changes at ORD suggest that PRE 3 first passed from north to south at ~1000 UTC 13 September and returned south to north by ~1400 UTC 13 September (Fig. 12f). A final period of significant precipitation occurs at ORD in association with a wind shift from southwesterly to northerly and a SLP decrease of ~4 hPa (Fig. 12g) as the western end of PRE 3 shifts southward between 1200 and 1800 UTC 14 September (Fig. 11e). The southward shift of PRE 3 occurs in conjunction with cold-air advection behind a deepening surface cyclone northeast of Lake Huron (Fig. 9d). Subsequent to 0600 UTC 14 September the western edge of PRE 3 merges with the TC Ike rain shield (Figs. 9d and 11e) along the aforementioned baroclinic zone, while the eastern edge of PRE 3 dissipates (not shown). The merger of PRE 3 and TC Ike on 14 September is also associated with sufficient CAPE values (>1000 J kg^{-1}) at Springfield (SGF), Missouri, to support convective precipitation within PRE 3 (Figs. 10f and 11e).

Temperature and dewpoint temperatures at ORD gradually decrease between 0000 and 1500 UTC 14 September as cooler air enters the northwest periphery of the TC Ike circulation (Fig. 12g). The arrival of this cooler air is seen in a meteogram from SGF at ~0600 UTC 14 September as winds shift from east-southeasterly to northerly with sustained heavy rain (Fig. 11h), at low levels (<850 hPa) in the sounding at ILX at 1200 UTC 14 September (Fig. 10f), and after 1200 UTC 14 September at WNC as winds shift to northwesterly below 4000 m and back with height above this level (Fig. 13d). The arrival of slightly cooler air in the northwest periphery of TC Ike is associated with heavy stratiform rain along and to the left of the TC track. In this context, the heavy rain along the lower-tropospheric baroclinic zone ahead of TC Ike is comparable to that

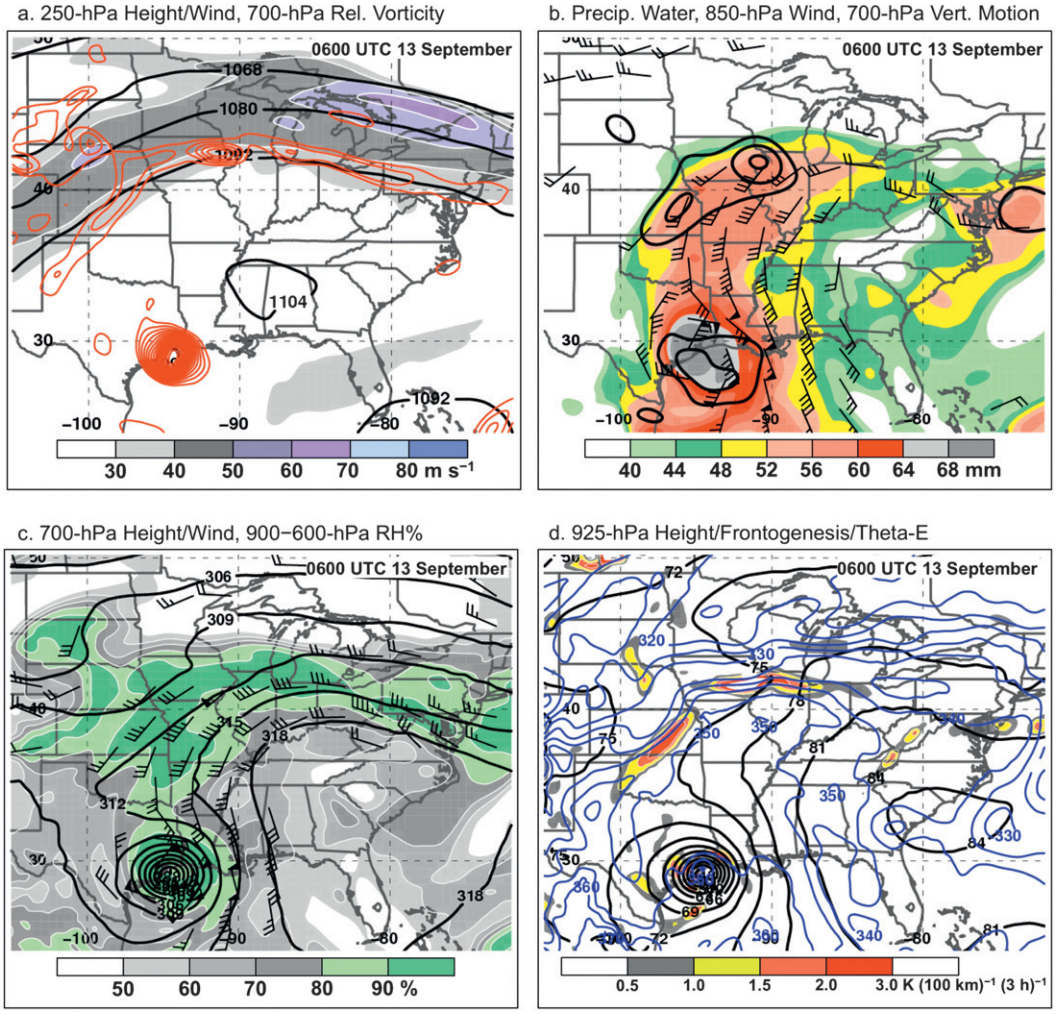

FIG. 14. Synoptic analysis at 0600 UTC 13 Sep 2008 of (a) 250-hPa geopotential height (solid black contours every 12 dam), wind speed (shaded according to the color bar and thin white contours every 10 m s^{-1}), and 700-hPa relative vorticity (solid red contours every 4.0×10^{-5} s^{-1} starting at 4.0×10^{-5} s^{-1}); (b) 850-hPa wind (pennant, full barb, and half barb denote 25.0, 5.0, and 2.5 m s^{-1}, respectively), 700-hPa ascent (solid black contours every 3.0×10^{-3} hPa s^{-1} starting at -3.0×10^{-3} hPa s^{-1}), and PW (shaded according to the color bar in mm); (c) 700-hPa geopotential height (solid black contours every 3 dam), wind (standard barbs in kt), and 900–600-hPa layer-averaged relative humidity (shaded according to the color bar in percent); and (d) 925-hPa geopotential height (solid black contours every 3 dam), equivalent potential temperature (solid blue contours every 5 K), and Petterssen frontogenesis [shaded according to the color bar in K (100 km)$^{-1}$ (3 h)$^{-1}$].

seen in TCs undergoing extratropical transition (ET) such as TC Floyd (1999; Atallah and Bosart 2003).

The organization and maturation of PRE 3 bear a resemblance to the organization and maturation of PREs that develop within the entrance region of anticyclonically curved (AC) upper-tropospheric jet streaks (i.e., AC PREs) studied by Galarneau et al. (2010). Synoptic-scale features documented by Galarneau et al. (2010, see their Figs. 5 and 8) critical for AC PRE development are also present during the maturation of PRE 3. As moisture from TC Ike arrives proximate PRE 3, a broad anticyclonically curved band of 700-hPa cyclonic vorticity extends from the Texas Panhandle to New Jersey along the anticyclonic shear side of the STJ at 0600 UTC 13 September (Fig. 14a). This anticyclonically curved band of lower-tropospheric relative vorticity is associated with a baroclinic zone located in the STJ equatorward entrance region and the location of PRE 3 (Figs. 11c and 14a). A 700-hPa closed anticyclone over the Southeast is helping to sustain an anticyclonically curved LLJ with a corridor of 20–25 m s^{-1} winds oriented perpendicular to the lower-tropospheric baroclinic zone over southern Iowa and northern Illinois (Fig. 14c). Tropical moisture (PW values >56 mm) is transported from TC Ike by the

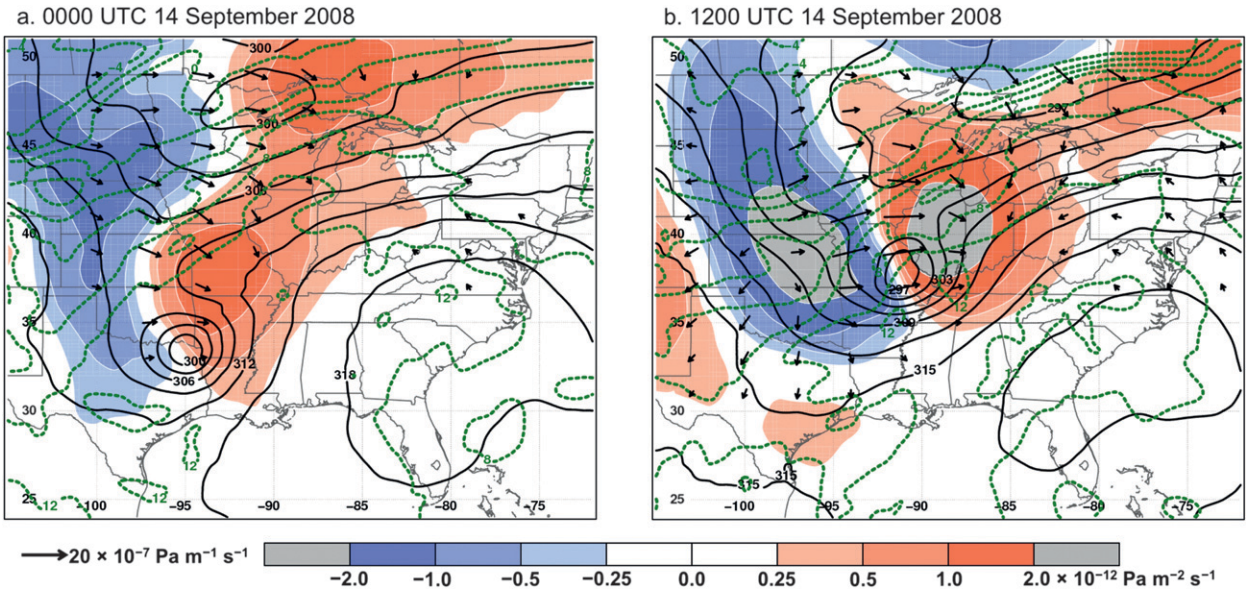

FIG. 15. The 700-hPa geopotential height (solid contours every 3 dam), temperature (dashed green contours every 2 K), **Q** vectors (arrows $>2.5 \times 10^{-7}$ Pa m^{-1} s^{-1}), and the right-hand-side of the **Q**-vector form of the QG omega equation (shaded according to the color bar in 10^{-12} Pa m^{-2} s^{-1}) at (a) 0000 UTC 14 Sep and (b) 1200 UTC 14 Sep 2008.

LLJ to a region of focused 700-hPa ascent associated with PRE 3 along the lower-tropospheric baroclinic zone (Figs. 14a,b). Ascent along the lower-tropospheric baroclinic zone occurs collocated with a band of high (>90%) layer-mean 900–600-hPa relative humidity (Fig. 14c), an east–west-oriented band of frontogenesis at 925 hPa along the warm side of the zonally oriented baroclinic zone (Fig. 14d), and the STJ equatorward entrance region (Figs. 9b,c and 14a).

Evidence for QG forcing for ascent during the maturation of PRE 3 on 14 September is illustrated by the 700-hPa geopotential height, temperature, **Q** vector, and **Q**-vector divergence at 0000 and 1200 UTC 14 September (Figs. 15a,b). As TC Ike approaches the lower Great Lakes and begins to interact with a trough over the upper Midwest, QG forcing for ascent increases to the northeast of the storm beneath the STJ equatorward entrance region (Figs. 9c,d and 15). The **Q** vectors oriented across the 700-hPa isotherms toward warmer air at 0000 and 1200 UTC 14 September along and ahead of PRE 3 and TC Ike indicate that frontogenetical forcing for ascent is helping to sustain heavy rainfall in the merged PRE 3 and TC Ike rain shield along the lower-tropospheric baroclinic zone ahead of TC Ike (Figs. 11e and 15).

6. Results: Interactions between PREs and the large-scale environment

The interaction of PREs 2 and 3 with the STJ between 0000 UTC 12 September and 0600 UTC 14 September is documented within a PV framework and makes use of cross-sectional and upper-tropospheric PV, streamfunction, nondivergent, and irrotational wind analyses (Figs. 16 and 17, respectively). The PV framework, in conjunction with nondivergent and irrotational wind analyses, is used to illustrate how changes in the magnitude of the upper-tropospheric PV gradient proximate to the STJ may result from the poleward advection of low PV air by the irrotational wind. In the present study, the poleward-directed irrotational wind is driven by deep moist convection and upper-tropospheric diabatic outflow associated with PREs 2 and 3 and TC Ike.

The maturation of PRE 2 (over Oklahoma and Kansas) and development of PRE 3 (over New Mexico and the Texas Panhandle) occurs in the STJ equatorward entrance region (cf. Figs. 9a,b) in association with weak upslope flow, midtropospheric ascent and warm-air advection, and deep moisture (water vapor mixing ratio) at 0000 UTC 12 September (Figs. 16a,b). In response to the associated deep moist convection (and corresponding corridor of high cloud cover) and upper-tropospheric diabatic outflow, the poleward-directed irrotational upper-tropospheric flow over mature PRE 2 and developing PRE 3 advects lower values of upper-tropospheric PV poleward along the axis of the STJ (Figs. 17a,b). Likewise, the developing midtropospheric ascent and frontogenesis over mature PRE 2 and developing PRE 3 is consistent with the previous AMA trajectory that shows lower-tropospheric (925 hPa) upslope flow in a moistening warm-air advection environment (Fig. 7b). Consequently,

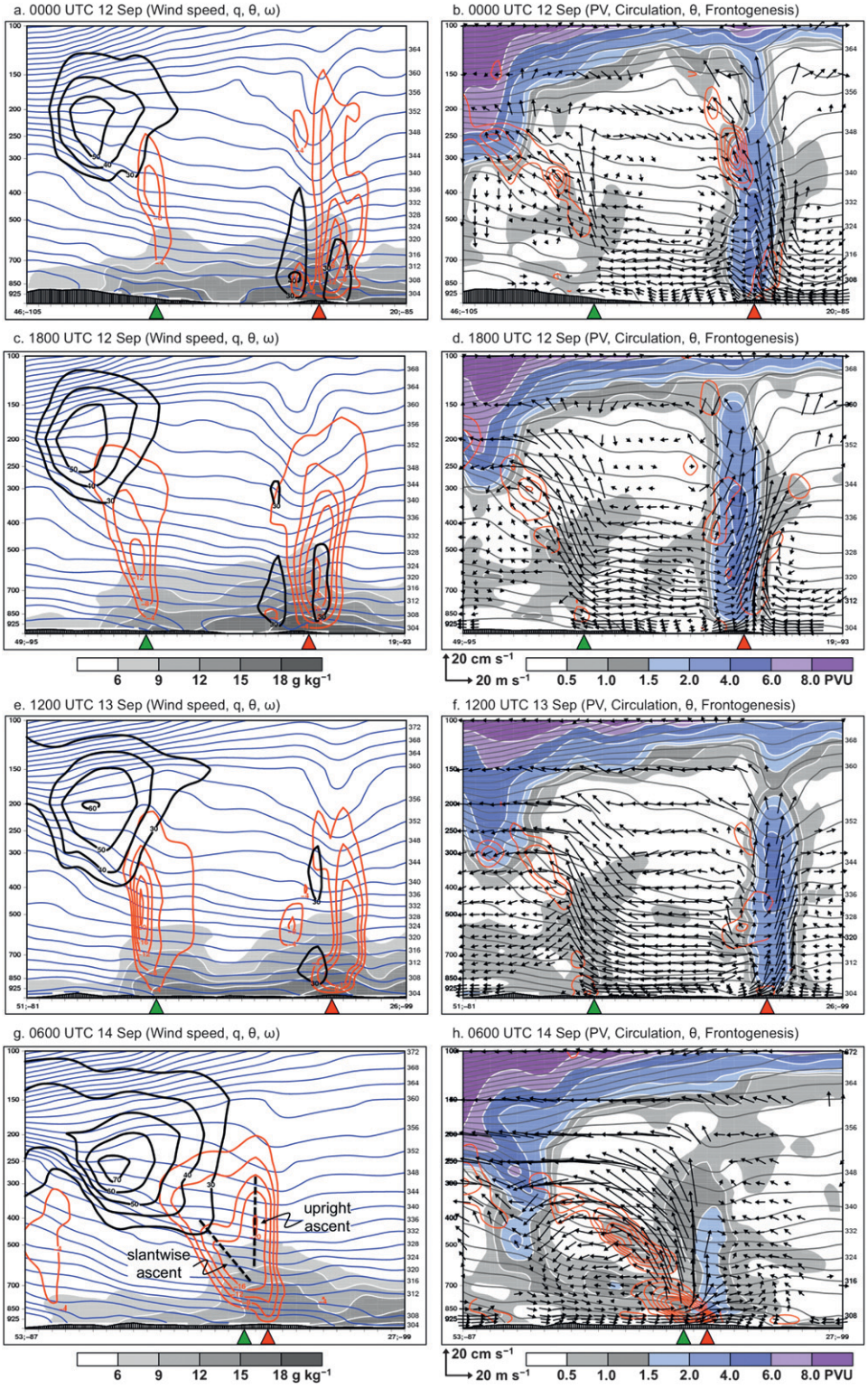
a. 0000 UTC 12 Sep (Wind speed, q, θ, ω)
b. 0000 UTC 12 Sep (PV, Circulation, θ, Frontogenesis)
c. 1800 UTC 12 Sep (Wind speed, q, θ, ω)
d. 1800 UTC 12 Sep (PV, Circulation, θ, Frontogenesis)
e. 1200 UTC 13 Sep (Wind speed, q, θ, ω)
f. 1200 UTC 13 Sep (PV, Circulation, θ, Frontogenesis)
g. 0600 UTC 14 Sep (Wind speed, q, θ, ω)
h. 0600 UTC 14 Sep (PV, Circulation, θ, Frontogenesis)
upright ascent
slantwise ascent
6 9 12 15 18 g kg−1
20 cm s−1
20 m s−1
0.5 1.0 1.5 2.0 4.0 6.0 8.0 PVU

the magnitude of the upper-tropospheric PV gradient and strength of the STJ increases from New Mexico to the Great Lakes by 1800 UTC 12 September (Figs. 17c,d).

The absorption of PRE 2 by developing PRE 3 occurs in the equatorward entrance region of the strengthened STJ in association with weak midtropospheric frontogenesis, deep ascent, and lower-tropospheric convergence at the nose of a water vapor mixing ratio maximum well poleward of the PV tower associated with TC Ike at 1800 UTC 12 September (Figs. 16c,d). The associated deep moist convection and upper-tropospheric diabatic outflow continues to advect lower values of upper-tropospheric PV by the irrotational flow poleward, resulting in a further increase in the magnitude of the upper-tropospheric PV gradient and strength of the STJ on the poleward side of the corridor of high cloud cover over the central plains and Great Lakes region (Figs. 17c,d). The previous DSM trajectory 6 h later (0000 UTC 13 September) supports the concentrated ascent in PRE 3 (Figs. 7c and 16c).

The maturation of PRE 3 by 1200 UTC 13 September is associated with the development of a weak column of 900–600-hPa PV in a baroclinic environment (Figs. 16e,f). This midtropospheric PV tower is collocated with a band of lower-tropospheric frontogenesis, deep ascent, veering winds with height, and a region of higher water vapor mixing ratio values, suggestive of deep moist convection (Figs. 16e,f). The horizontally confined region of deep ascent and the quasi-horizontal flow in the plane of the cross section is consistent with the previous BEH trajectory analysis that shows little net vertical displacement of air parcels until they reach the frontogenetic circulation of the lower-tropospheric baroclinic zone associated with PRE 3 (Fig. 7e). PRE 3 matures in a separate region from the deep warm-core TC Ike PV tower and remains located in the equatorward entrance region of an intense 60 m s^{-1} STJ (Fig. 16f). The associated deep moist convection and upper-tropospheric diabatic outflow over PRE 3 continues to advect lower values of upper-tropospheric PV poleward across the central and eastern Great Lakes (sharpening the PV ridge) and along the axis of the STJ at 1200 UTC 13 September (Figs. 17e,f).

The merger of TC Ike with the western portion of PRE 3 at 0600 UTC 14 September is manifest by a deep warm-core PV tower and upright ascent between 850 and 300 hPa associated with TC Ike and a separate sloped corridor of high PV and sloped ascent between 850 and 300 hPa associated with PRE 3 (Figs. 16g,h). The sloped corridor of high PV and sloped ascent is associated with strong frontogenesis and suggests the development of an upper-tropospheric front in the equatorward entrance region of the STJ, consistent with continued STJ intensification (Figs. 16g,h). Although deep upright ascent suggests that the TC Ike PV tower is separate from the region of sloped ascent and frontogenesis farther north, mid-to-upper-tropospheric diabatic heating associated with TC Ike is probably enhancing baroclinicity in support of the sloped ascent and frontogenesis in the equatorward entrance region of the STJ (Figs. 16g,h). The indicated vigor of the ascent tower associated with TC Ike at 0600 UTC 14 September is consistent with the previous SGF trajectory that shows deep ascent is concentrated near TC Ike (Figs. 7g and 16g).

The merger of TC Ike with the western portion of PRE 3 at 0600 UTC 14 September is also associated with the ET of TC Ike and an interaction of the TC with an upper-tropospheric trough to the west (Figs. 17g,h). The upper-tropospheric ridge poleward of TC Ike amplifies where the divergent irrotational flow is strongest and the advection of low PV air by the irrotational wind is largest from Nebraska to Wisconsin (Figs. 17g,h). Upper-tropospheric ridge amplification, poleward low-PV advection by the irrotational wind, and associated STJ intensification occur along the northern edge of the corridor of high cloud cover and are suggestive of the importance of the cumulative upscale effects of persistent diabatic heating on the reconfiguration of the upper-tropospheric flow downstream of the PREs and TC Ike (Figs. 17g,h).

A continuity map showing the evolution of the layer-mean 300–200-hPa PV field based upon once daily (1200 UTC) observations for 11–14 September illustrate

←

FIG. 16. Vertical cross-sectional analysis of (left) water vapor mixing ratio (shaded in g kg^{-1} according to the color bar), potential temperature (contoured in blue every 4 K), ascent (contoured in red every 5×10^{-3} hPa s^{-1} starting at -5×10^{-3} hPa s^{-1}), and wind speed (contoured in black every 10 m s^{-1} starting at 30 m s^{-1}) every 18 h at (a) 0000 UTC 12 Sep, (c) 1800 UTC 12 Sep, (e) 1200 UTC 13 Sep, and (g) 0600 UTC 14 Sep 2008. (right) Potential vorticity [shaded in potential vorticity unit (PVU) according to the color bar, where 1 PVU = 10^{-6} K m^2 kg^{-1} s^{-1}]. Petterssen frontogenesis [contoured in red every 1 K $(100\ km)^{-1}$ $(3\ h)^{-1}$ starting at 1 K $(100\ km)^{-1}$ $(3\ h)^{-1}$], potential temperature (contoured in gray every 4 K), and the flow (circulation) in the plane of the cross section (vectors) every 18 h at (b) 0000 UTC 12 Sep, (d) 1800 UTC 12 Sep, (f) 1200 UTC 13 Sep, and (h) 0600 UTC 14 Sep 2008. The green (red) triangle marks the position of the PRE (TC). Cross-sectional lines are drawn in Fig. 17.

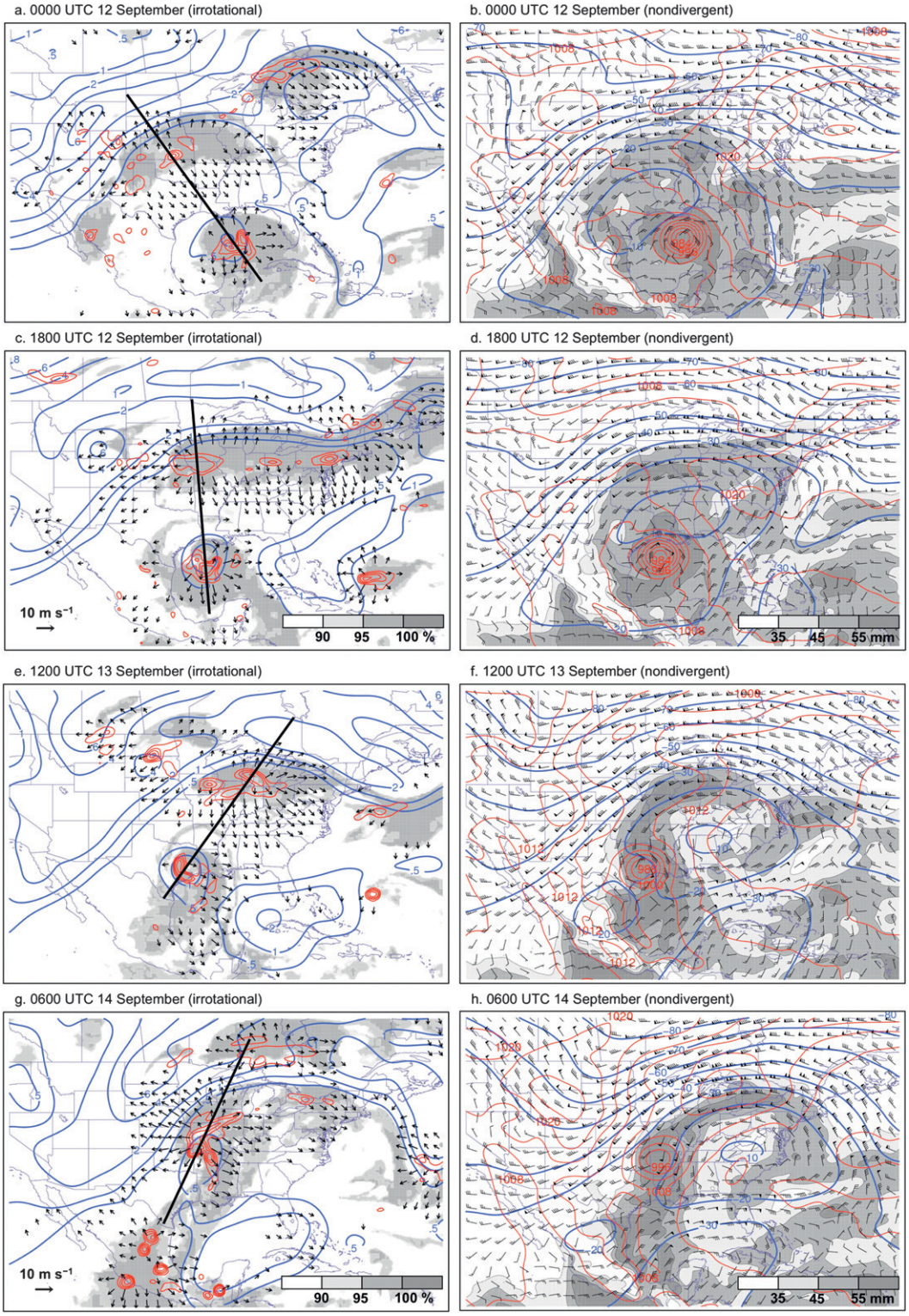
a. 0000 UTC 12 September (irrotational)
b. 0000 UTC 12 September (nondivergent)
c. 1800 UTC 12 September (irrotational)
d. 1800 UTC 12 September (nondivergent)
e. 1200 UTC 13 September (irrotational)
f. 1200 UTC 13 September (nondivergent)
g. 0600 UTC 14 September (irrotational)
h. 0600 UTC 14 September (nondivergent)
10 m s−1
90 95 100 %
35 45 55 mm

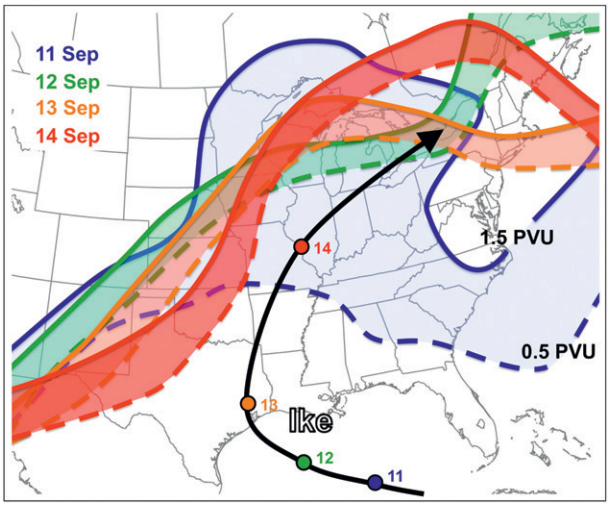

FIG. 18. Schematic representation of 300–200-hPa layer-mean PV shaded between the 0.5 PVU (dashed) and 1.5 PVU (solid) contours at 1200 UTC 11 Sep (blue), 12 Sep (green), 13 Sep (orange), and 14 Sep (red). The 1200 UTC positions of TC Ike are shown for 11–14 Sep 2008.

the large-scale PV reconfiguration over the CONUS from PRE- and Ike-influenced diabatically driven downstream ridge building and STJ intensification (Fig. 18). The PV gradient strengthens noticeably across the upper Midwest and Great Lakes in the 24 h ending 1200 UTC 12 September and then strengthens eastward as the PV pattern becomes more "wavelike" and amplified by 1200 UTC 13 September. The PV gradient further strengthens and the PV wave pattern further amplifies by 1200 UTC 14 September in association with a shortening of the downstream half wavelength of the 300–200-hPa trough–ridge couplet over the southern plains and Great Lakes region. The shortening of the downstream half wavelength occurs in response to the accumulated effects of the diabatically driven upper-tropospheric outflow from the three PREs and TC Ike in conjunction with the approach of an upstream trough and continued downstream ridge building (Figs. 9c,d; 15a,b; and 17g,h). At 0000 and 1200 UTC 14 September, lower-tropospheric cold-air advection over the northern plains likely contributes to the deepening of the upstream trough and downstream ridge building by enhancing differential cyclonic vorticity advection by the thermal wind and increasing QG forcing for ascent over the lower Great Lakes (manifest as an increase in **Q**-vector convergence for ascent; Figs. 15a,b).

7. Conclusions

The focus of this paper was on three PREs that occurred over the southern plains and Midwest in advance of TCs Lowell and Ike during 10–15 September 2008. The PREs combined to produce all-time daily record rainfall totals at LBB, ICT, and ORD. While previous literature has documented the crucial synoptic- and mesoscale ingredients leading to the development and maturation of PREs in advance of western North Atlantic TCs, this paper highlights the influence of multiple TCs and moisture sources on PRE development and maturation and the interaction of PREs with the large-scale environment.

Overview schematics of the three PREs are provided in Fig. 19 to summarize the moisture sources for each PRE and continuity among the three PREs. PRE 1 (Fig. 19a) organized over Texas in association with moisture from a stalled front and the disturbance in the Bay of Campeche, and matured in association with mid-to-upper-tropospheric moisture from TC Lowell. PRE 1 developed along the southern edge of a weakly frontogenetic baroclinic zone, downstream of a weak 700-hPa trough, and in the equatorward entrance region of a weak STJ. PRE 2 (Fig. 19b) organized over the Texas Panhandle in association with moisture from the disturbance in the Bay of Campeche and TC Lowell, and matured over Kansas, Oklahoma, and Missouri. Although PRE 2 formed along the same quasi-stationary frontogenetic baroclinic zone as PRE 1, the observed precipitation totals were larger as the PRE was influenced by a more prolonged period of lower-tropospheric tropical moisture transport from the Bay of Campeche up the Rio Grande Valley and mid-to-upper-tropospheric tropical moisture transport from TC Lowell. PRE 2 also matured in the equatorward entrance region of an intensifying STJ from New Mexico to Nebraska in association with deep convection over TC Lowell and PRE 2.

←

FIG. 17. (left) The 300–200-hPa layer-mean PV (solid blue contours at 0.5, 1.0, 2.0, 4.0, and 6.0 PVU) and irrotational wind (vectors starting at 3.75 m s^{-1}), 600–400-hPa layer-mean ascent (solid red contours every 5×10^{-3} hPa s^{-1}), and fractional "high" cloud cover (shaded according to the grayscale in %) at every 18 h at (a) 0000 UTC 12 Sep, (c) 1800 UTC 12 Sep, (e) 1200 UTC 13 Sep, and (g) 0600 UTC 14 Sep 2008. (right) 300–200-hPa layer-mean streamfunction (solid blue contours every 10×10^6 m^2 s^{-1}) and nondivergent wind (pennant, full barb, and half barb denote 25.0, 5.0, and 2.5 m s^{-1}, respectively), sea level pressure (solid red contours every 4 hPa), and PW (shaded according to the grayscale in mm) every 18 h at (b) 0000 UTC 12 Sep, (d) 1800 UTC 12 Sep, (f) 1200 UTC 13 Sep, and (h) 0600 UTC 14 Sep 2008. (left) Cross-sectional lines for Fig. 16 are shown. Fractional high cloud cover is derived from the 0.25° Year of Tropical Convection (YOTC) dataset accessible online at http://data-portal.ecmwf.int/data/d/yotc_od/.

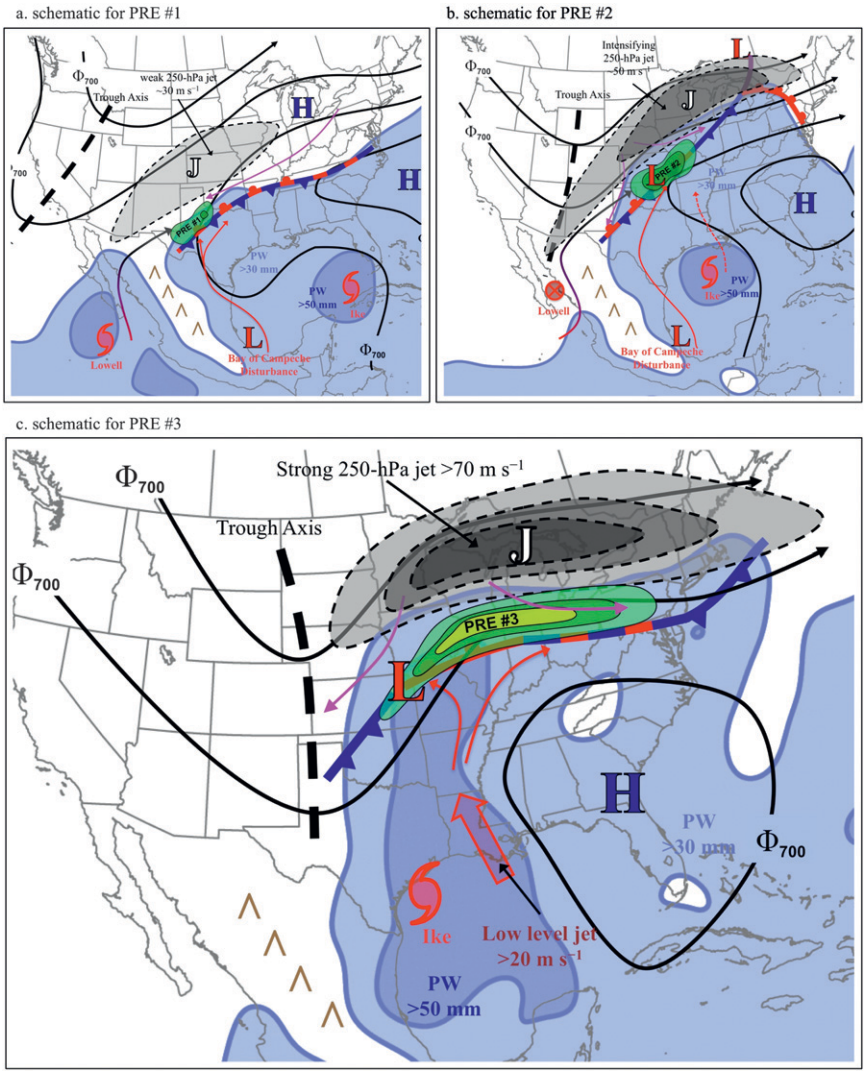

FIG. 19. Overview schematics for the meteorological features associated with (a) PRE 1, (b) PRE 2, and (c) PRE 3. Figure depicts 1) location and intensity of PREs (green-to-yellow shading), 2) 250-hPa jet (''J''; gray shading and thin dashed contours), 3) 700-hPa trough axis (thick dashed black line) and height contours (solid black contours), 4) lower-tropospheric jet [large red arrow in (c)], 5) tropospheric moisture (light and dark blue shading representing precipitable water values >30 and >50 mm, respectively), 6) tropical features (Ike: TC symbol, Lowell: TC and TD symbols, Bay of Campeche disturbance: ''L''), 7) surface frontal features, 8) lower-tropospheric wind pattern near the frontal boundary and PRE in the warm (red-arrowed lines) and cool (magenta-arrowed lines) air, and 9) surface cyclone and anticyclone locations given by the red ''L'' and blue ''H'' symbols, respectively.

PREs 1 and 2 form more than 1000 km from the Bay of Campeche disturbance, TC Lowell, and TC Ike. The large separation distance between the tropical features and PREs suggests that the direct dynamical influence of the tropical features on the development of the PREs is likely small.

PRE 3 (Fig. 19c) organized over northern Mexico and southwestern Texas and merged with PRE 2 over the central plains. The dominant moisture source for the maturation of PRE 3 is TC Ike in conjunction with a strong LLJ between TC Ike and a 700-hPa ridge over the Southeast. PRE 3 forms along a lower-tropospheric frontogenetic baroclinic zone in a region of confluent flow beneath the equatorward entrance region of a strong STJ that is intensifying in part due to the diabatically driven outflow from PRE 3. The large separation distance >1000 km between TC Ike and PRE 3 suggests that the direct dynamical influence of the TC on the development of the PRE is likely small. TC Ike

is too far the from the lower-tropospheric baroclinic zone and embedded PRE 3 to directly influence the magnitude of the warm-air advection and associated frontogenesis, and the diabatically driven upper-tropospheric outflow from TC Ike does not extend far enough poleward to initially influence the strength of the STJ.

The three PREs contained several ingredients common to AC PRE development identified by Galarneau et al. (2010), including formation in an equatorward jet-entrance region, on the western flank of a lower-tropospheric anticyclone, to the east of a midtropospheric trough, and along a frontogenetic lower-tropospheric baroclinic zone in the presence of deep tropical moisture from a distant TC. The development of the PREs in the equatorward entrance region of the upper-tropospheric STJ is reminiscent of notable PREs with TC Rita (2005; Moore 2010), TC Erin (2007; Galarneau et al. 2010), and TC Agnes (1972; Bosart and Carr 1978; Bosart and Dean 1991). This flow configuration has also been shown to favor extreme rain-producing MCSs (e.g., Maddox et al. 1979; Heideman and Fritsch 1988; Kunkel et al. 1993; Trier and Parsons 1993; Augustine and Caracena 1994; Konrad 1997; Junker et al. 1999; Moore et al. 2003; Schumacher and Johnson 2005, 2006; Trier et al. 2006; Ashley and Ashley 2008). The three PREs were noticeably similar to quasi-stationary long-lived ''training line–adjoining stratiform'' extreme rain-producing MCSs documented by Schumacher and Johnson (2005).

The PREs develop in an environment that is preconditioned for heavy rainfall by the presence of deep moisture, lower-tropospheric frontogenesis, lower- and midtropospheric warm advection, and upper-tropospheric divergence in the STJ equatorward entrance region. The overview schematics for the three PREs emphasize the large separation distances (>1000 km) between the PREs and TCs, indicating that the dynamical influence of the TCs on the PREs is likely small. The role of the TCs in producing the PRE is mainly indirect: the TC serves primarily as a source of deep tropical moisture (Moore 2010). The overview schematics demonstrate that each PRE is successively stronger than its predecessor, likely associated with the intensifying STJ, strengthening lower-tropospheric baroclinic zone, and the cumulative upscale effect of persistent deep convection associated with the PREs on the large-scale flow.

The cumulative upscale effect of persistent deep convection associated with the three PREs enhanced and ''locked in'' a strong, quasi-stationary upper-tropospheric closed anticyclone over the Ohio Valley and produced a back-building and intensifying STJ over the upper Midwest and northern Great Lakes. As the eastward-advancing deep trough over the Southwest, which permitted tropical moisture from TC Lowell to be advected northeastward, encountered the quasi-stationary diabatically enhanced anticyclone to the east, the distance between the upstream trough axis and the downstream ridge axis decreased. This shortening of the half-wavelength of the trough–ridge pattern was associated with increased QG forcing for ascent that contributed to the maturation of PRE 3 and the subsequent ET of TC Ike. Bosart and Lackmann (1995), in their analysis of the reintensification of TC David (1979) over the Northeast, and Dickinson et al. (1997) and Bosart (1999), in their analysis of the March 1993 ''Superstorm'' over eastern North America, pointed to the dynamical importance of the shortening of the downstream half wavelength due to diabatically driven synoptic-scale ridging and jet stream intensification in augmenting QG forcing for ascent over cyclone centers during cyclogenesis. The observed diabatic influence of the PREs on downstream ridge amplification is comparable to the synoptic-scale feedback from diabatic heating associated with heavy precipitation accompanying tropical convection (e.g., Sardeshmukh and Hoskins 1988), MCSs (e.g.; Fritsch and Maddox 1981; Chen et al. 2006; Saulo et al. 2007; Metz and Bosart 2010), recurving and transitioning TCs (e.g., Bosart and Lackmann 1995; Atallah and Bosart 2003; Riemer et al. 2008; Torn and Hakim 2009; Archambault 2010; Riemer and Jones 2010), extratropical cyclones (e.g., Dickinson et al. 1997; Bosart 1999; Pomroy and Thorpe 2000; Archambault et al. 2010), and positively tilted PV streamers (e.g., Massacand et al. 2001).

The analysis of the development of multiple PREs in this study suggests that high-impact flood-producing mesoscale rainstorms ahead of TCs can occur in association with multiple moisture source regions. The current analysis, however, does not identify whether PRE development would have occurred independent of individual moisture source regions associated with the stalled frontal boundary, the Bay of Campeche disturbance, TC Lowell, or TC Ike. Given that each PRE was successively more intense than the previous PRE, and that each PRE successively contributed to an intensification of the STJ, it is possible to speculate that the later PREs may have been less intense in the absence of the earlier PREs. Future work will investigate PREs using high-resolution numerical simulations to quantitatively assess the contributions of multiple moisture source regions to PRE development, the predictability of multiple interacting PREs, and the importance of the cumulative upscale effect of persistent deep convection on the evolution of the STJ and PRE development.

Acknowledgments. The authors thank David Roth at NCEP/HPC, Sheldon Kusselson at NOAA/NESDIS, and Greg Tripoli at the University of Wisconsin—Madison

for stimulating conversations about PREs. The authors thank Russ Schumacher (Colorado State University) and an anonymous reviewer for comments that helped to clarify and improve the manuscript. The authors also thank Anantha Aiyyer (North Carolina State University) for developing software to calculate air parcel trajectories, and Dave Vollaro (University at Albany, SUNY) for help in obtaining and processing the TRMM satellite data. Research support was provided by NSF Grant ATM-0849491 and NOAA/CSTAR Grant NA07NWS4680001.

REFERENCES

Archambault, H. M., 2010: Large-scale flow reconfigurations over North America associated with recurving western North Pacific tropical cyclones. Preprints, *29th Conf. on Hurricanes and Tropical Meteorology,* Tucson, AZ, Amer. Meteor. Soc., 1D.2. [Available online at http://ams.confex.com/ams/29Hurricanes/techprogram/paper_169099.htm.]

——, D. Keyser, and L. F. Bosart, 2010: Relationships between large-scale regime transitions and major cool-season precipitation events in the northeastern United States. *Mon. Wea. Rev.,* **138,** 3454–3473.

Ashley, S. T., and W. S. Ashley, 2008: Flood fatalities in the United States. *J. Appl. Meteor. Climatol.,* **47,** 805–818.

Atallah, E. H., and L. F. Bosart, 2003: The extratropical transition and precipitation distribution of Hurricane Floyd (1999). *Mon. Wea. Rev.,* **131,** 1063–1081.

Augustine, J. A., and F. Caracena, 1994: Lower-tropospheric precursors to nocturnal MCS development over the central United States. *Wea. Forecasting,* **9,** 116–135.

Bosart, L. F., 1999: Observed cyclone life cycles. *The Life Cycles of Extratropical Cyclones,* M. A. Shapiro and S. Grønås, Eds., Amer. Meteor. Soc., 187–213.

——, and F. H. Carr, 1978: A case study of excessive rainfall centered around Wellsville, New York, 20–21 June 1972. *Mon. Wea. Rev.,* **106,** 348–362.

——, and D. B. Dean, 1991: The Agnes rainstorm of June 1972: Surface feature evolution culminating in inland storm redevelopment. *Wea. Forecasting,* **6,** 515–537.

——, and G. M. Lackmann, 1995: Postlandfall tropical cyclone reintensification in a weakly baroclinic environment: A case study of Hurricane David (September 1979). *Mon. Wea. Rev.,* **123,** 3268–3291.

Chen, G. T.-J., C.-C. Wang, and L.-F. Lin, 2006: A diagnostic study of a retreating mei-yu front and the accompanying low-level jet formation and intensification. *Mon. Wea. Rev.,* **134,** 874–896.

Cote, M. R., 2007: Predecessor rain events in advance of tropical cyclones. M.S. thesis, Department of Atmospheric and Environmental Sciences, University at Albany, State University of New York, Albany, NY, 198 pp.

Dickinson, M. J., L. F. Bosart, W. E. Bracken, G. J. Hakim, D. M. Schultz, M. A. Bedrick, and K. R. Tyle, 1997: The March 1993 Superstorm cyclogenesis: Incipient phase synoptic- and convective-scale flow interaction and model performance. *Mon. Wea. Rev.,* **125,** 3041–3072.

Fritsch, J. M., and R. A. Maddox, 1981: Convectively driven mesoscale weather systems aloft. Part I: Observations. *J. Appl. Meteor.,* **20,** 9–19.

Galarneau, T. J., Jr., L. F. Bosart, and R. S. Schumacher, 2010: Predecessor rain events ahead of tropical cyclones. *Mon. Wea. Rev.,* **138,** 3272–3297.

Hart, R. E., and R. H. Grumm, 2001: Using normalized climatological anomalies to rank synoptic-scale events objectively. *Mon. Wea. Rev.,* **129,** 2426–2442.

Heideman, K. F., and J. M. Fritsch, 1988: Forcing mechanisms and other characteristics of significant summertime precipitation. *Wea. Forecasting,* **3,** 115–130.

Huffman, G. J., and Coauthors, 2007: The TRMM Multisatellite Precipitation Analysis (TMPA): Quasi-global, multiyear, combined-sensor precipitation estimates at fine scales. *J. Hydrometeor.,* **8,** 38–55.

Junker, N. W., R. S. Schneider, and S. L. Fauver, 1999: A study of heavy rainfall events during the Great Midwest Flood of 1993. *Wea. Forecasting,* **14,** 701–712.

Kalnay, E., and Coauthors, 1996: The NCEP/NCAR 40-Year Reanalysis Project. *Bull. Amer. Meteor. Soc.,* **77,** 437–472.

Konrad, C. E., 1997: Synoptic-scale features associated with warm season heavy rainfall over the interior southeastern United States. *Wea. Forecasting,* **12,** 557–571.

Kunkel, K. E., S. A. Changnon, and R. T. Shealy, 1993: Temporal and spatial characteristics of heavy-precipitation events in the Midwest. *Mon. Wea. Rev.,* **121,** 858–866.

Maddox, R. A., C. F. Chappel, and L. R. Hoxit, 1979: Synoptic and meso-alpha scale aspects of flash-flood events. *Bull. Amer. Meteor. Soc.,* **60,** 115–123.

Massacand, A. C., H. Wernli, and H. C. Davies, 2001: Influence of upstream diabatic heating upon an Alpine event of heavy precipitation. *Mon. Wea. Rev.,* **129,** 2822–2828.

Metz, N. D., and L. F. Bosart, 2010: Derecho and MCS development, evolution, and multiscale interactions during 3–5 July 2003. *Mon. Wea. Rev.,* **138,** 3048–3070.

Moore, B. J., 2010: Synoptic-scale environments and dynamical mechanisms associated with predecessor rain events ahead of tropical cyclones. M.S. thesis, Department of Atmospheric and Environmental Sciences, University at Albany, State University of New York, Albany, NY, 150 pp.

——, P. J. Neiman, F. M. Ralph, and F. E. Barthold, 2012: Physical processes associated with heavy flooding rainfall in Nashville, Tennessee, and vicinity during 1–2 May 2010: The role of an atmospheric river and mesoscale convective systems. *Mon. Wea. Rev.,* **140,** 358–378.

Moore, J. T., F. H. Glass, C. E. Graves, S. M. Rochette, and M. J. Singer, 2003: The environment of warm-season elevated thunderstorms associated with heavy rainfall over the central United States. *Wea. Forecasting,* **18,** 861–878.

Neiman, P. J., F. M. Ralph, G. A. Wick, J. Lundquist, and M. D. Dettinger, 2008: Meteorological characteristics and overland precipitation impacts of atmospheric rivers affecting the West Coast of North America based on eight years of SSM/I satellite observations. *J. Hydrometeor.,* **9,** 22–47.

Pomroy, H. R., and A. J. Thorpe, 2000: The evolution and dynamical role of reduced upper-tropospheric potential vorticity in Intensive Observing Period One of FASTEX. *Mon. Wea. Rev.,* **128,** 1817–1834.

Riemer, M., and S. C. Jones, 2010: The downstream impact of tropical cyclones on a developing baroclinic wave in idealized scenarios of extratropical transition. *Quart. J. Roy. Meteor. Soc.,* **136,** 617–637.

——, ——, and C. A. Davis, 2008: The impact of extratropical transition on the downstream flow: An idealized modeling study with a straight jet. *Quart. J. Roy. Meteor. Soc.,* **134,** 69–91.

Sardeshmukh, P. D., and B. J. Hoskins, 1988: The generation of global rotational flow by steady idealized tropical divergence. *J. Atmos. Sci.,* **45,** 1228–1251.

Saulo, C., J. Ruiz, and Y. G. Skabar, 2007: Synergism between the low-level jet and organized convection at its exit region. *Mon. Wea. Rev.,* **135,** 1310–1326.

Schumacher, R. S., and R. H. Johnson, 2005: Organization and environmental properties of extreme-rain-producing mesoscale convective systems. *Mon. Wea. Rev.,* **133,** 961–976.

——, and ——, 2006: Characteristics of U.S. extreme rain events during 1999–2003. *Wea. Forecasting,* **21,** 69–85.

——, T. J. Galarneau Jr., and L. F. Bosart, 2011: Distant effects of a recurving tropical cyclone on rainfall in a midlatitude convective system: A high-impact predecessor rain event. *Mon. Wea. Rev.,* **139,** 650–667.

Torn, R. D., and G. J. Hakim, 2009: Initial condition sensitivity of western Pacific extratropical transitions determined using ensemble-based sensitivity analysis. *Mon. Wea. Rev.,* **137,** 3388–3406.

Trier, S. B., and D. B. Parsons, 1993: Evolution of environmental conditions preceding the development of a nocturnal mesoscale convective complex. *Mon. Wea. Rev.,* **121,** 1078–1098.

——, C. A. Davis, D. A. Ahijevych, M. L. Weisman, and G. H. Bryan, 2006: Mechanisms supporting long-lived episodes of propagating nocturnal convection within a 7-day WRF model simulation. *J. Atmos. Sci.,* **63,** 2437–2461.